Please cite this article in press as: Fan et al., Natural variations of *HvSRN1* modulate the spike rachis node number in barley, Plant Communications (2023), https://doi.org/10.1016/j.xplc.2023.100670

Plant Communications
Research article

CellPress
Partner Journal

Natural variations of *HvSRN1* modulate the spike rachis node number in barley

Chaofeng Fan[1,2], Dongdong Xu[1,3], Chunchao Wang[1], Zhaoyan Chen[1], Tingyu Dou[1], Dandan Qin[5], Aikui Guo[1], Meng Zhao[1], Honghong Pei[1], Mengwei Zhao[1], Renxu Zhang[1], Ke Wang[1], Jing Zhang[1], Zhongfu Ni[4,*] and Ganggang Guo[1,*]

[1]Key Laboratory of Grain Crop Genetic Resources Evaluation and Utilization (MARA), The National Key Facility for Crop Gene Resources and Genetic Improvement, Institute of Crop Sciences, Chinese Academy of Agricultural Sciences (ICS-CAAS), Beijing 100081, China

[2]Hainan Yazhou Bay Seed Laboratory, Sanya 572025, China

[3]Institute of Industrial Crops, Shandong Academy of Agricultural Sciences, Jinan 250100, China

[4]Key Laboratory of Crop Heterosis and Utilization, Beijing Key Laboratory of Crop Genetic Improvement, China Agricultural University, Beijing 100193, China

[5]Key Laboratory for Crop Molecular Breeding of Ministry of Agriculture and Rural Affairs, Institute of Food Crops, Hubei Academy of Agricultural Sciences, Wuhan 430064, China

***Correspondence: Zhongfu Ni (nizf@cau.edu.cn), Ganggang Guo (guoganggang@caas.cn)**

https://doi.org/10.1016/j.xplc.2023.100670

ABSTRACT

Grain number, one of the major determinants of yield in Triticeae crops, is largely determined by spikelet number and spike rachis node number (SRN). Here, we identified three quantitative trait loci (QTLs) for SRN using 145 recombinant inbred lines derived from a barley R90/1815D cross. *qSRN1*, the major-effect QTL, was mapped to chromosome 2H and explained up to 38.77% of SRN variation. Map-based cloning revealed that *qSRN1* encodes the RAWUL domain-containing protein HvSRN1. Further analysis revealed that two key SNPs in the *HvSRN1* promoter region (~2 kb upstream of the transcription start site) affect the transcript level of *HvSRN1* and contribute to variation in SRN. Similar to its orthologous proteins OsLAX2 and ZmBA2, HvSRN1 showed protein–protein interactions with HvLAX1, suggesting that the LAX2–LAX1 model for spike morphology regulation may be conserved in Poaceae crops. CRISPR-Cas9-induced *HvSRN1* mutants showed reduced SRN but increased grain size and weight, demonstrating a trade-off effect. Our results shed light on the role of *HvSRN1* variation in regulating the balance between grain number and weight in barley.

Key words: barley, fine-mapping, grain number, kernel weight

Fan C., Xu D., Wang C., Chen Z., Dou T., Qin D., Guo A., Zhao M., Pei H., Zhao M., Zhang R., Wang K., Zhang J., Ni Z., and Guo G. (2023). Natural variations of *HvSRN1* modulate the spike rachis node number in barley. Plant Comm. **4**, 100670.

INTRODUCTION

As a broadly adapted and stress-resistant cereal crop, barley (*Hordeum vulgare* L.) is widely used for feed, malt, and food (Harwood, 2019). Maintaining and enhancing barley production is important for the growing global population. The yield of cereal crops is generally determined by spike number per unit area, grain number per spike, and grain weight (Sakuma and Schnurbusch, 2020). The genetic basis of grain weight in cereal crops has been analyzed extensively (Zuo and Li., 2014; Li and Yang, 2017; Liu et al., 2017; Li et al., 2018; Ying et al., 2018; Thabet et al., 2020; Chen et al., 2021). Spike development begins with differentiation and growth of the spike inflorescence and ends with spikelet formation and seed production (Kirby, 1977; Kirby and Appleyard, 1980; 1984; Koppolu and Schnurbusch, 2019; Chen et al., 2022). In Triticeae crops, the inflorescence consists of a compact spike containing the main rachis, with a series of stalkless spikelets attached to each rachis internode.

Numerous genes that control grains per spike have been identified in rice and maize because of their economic importance. Most of these genes affect grain number by coordinating cell proliferation or expansion and are involved in signaling pathways of transcriptional regulatory factors, phytohormones, or other undefined factors. Transcription factors such as rice *IDEAL PLANT ARCHITECTURE1* (*IPA1*) (Jiao et al., 2010), *FRIZZY PANICLE*

Published by the Plant Communications Shanghai Editorial Office in association with Cell Press, an imprint of Elsevier Inc., on behalf of CSPB and CEMPS, CAS.

Please cite this article in press as: Fan et al., Natural variations of *HvSRN1* modulate the spike rachis node number in barley, Plant Communications (2023), https://doi.org/10.1016/j.xplc.2023.100670

(*FZP*) (Komatsu et al., 2003), and *REGULATOR OF GRAIN NUMBER1* (*RGN1*) (Li et al., 2022) influence grain number by regulating genes associated with inflorescence development. Cytokinin (CK) has key roles in regulating cell division and meristem activity in plants (Yang et al., 2021). Downregulation of *Grain Number1a* (*GN1a*)/*Cytokinin Oxidase 2* (*OsCKX2*) increased CK accumulation in the inflorescence meristem (IM), which increased grain number in rice (Yeh et al., 2015; Tu et al., 2022). As in rice, knockdown of *HvCKX1* or *HvCKX2* in barley also increased endogenous CK levels, and *ckx1* and *ckx2* lines exhibited increased spikelet number and total grain yield (Zalewski et al., 2012; Gasparis et al., 2019). *DROUGHT AND SALT TOLERANCE* (*DST*), which encodes a zinc-finger transcription factor, negatively regulates grain number by enhancing expression of *OsCKX2* in rice (Li et al., 2013). Genes involved in the DST–CKX pathway, such as *GRAIN SIZE AND NUMBER1* (*GSN1*) (Guo et al., 2018), *ERECTA1* (*OsER1*) (Guo et al., 2020), and *OsMED25* (Lin et al., 2022), have also been shown to regulate grain number.

Gibberellins (GAs) affect rice panicle architecture by antagonizing CK in maintaining IM activity, and *Knotted1-like Homeobox* (*KNOX*) acts as a coordinator between these two hormones (Su et al., 2021). Increased expression of *Grain Number per Panicle1* (*GNP1*) enhanced the expression of GA catabolism genes and *KNOX*, resulting in lower GA levels and increased CK activity, thereby increasing rice grain number (Wu et al., 2016).

Genes related to auxin biosynthesis, transport, and signaling also play critical roles in IM development (Goetz et al., 2021). In rice, *PLANT ARCHITECTURE AND YIELD1* (*PAY1*) and *Narrow leaf 1* (*NAL1*) are involved in the polar transport of auxin, thereby affecting grain number (Zhao et al., 2015; Lin et al., 2019). Maize *Barren inflorescence1* (*BIF1*) and *BIF4*, which encode auxin/indole-3-acetic acid (Aux/IAA) proteins, regulate the early stages of inflorescence formation by participating in the auxin signaling pathway to dynamically modulate expression of *Barren stalk1* (*BA1*), an ortholog of rice *LAX PANICLE1* (*LAX1*) (Galli et al., 2015). Both *OsLAX1* and *ZmBA1* are expressed in a narrow boundary region between the initiating axillary meristem (AM) and the shoot apical meristem and are core factors in AM generation (Skirpan et al., 2008; Oikawa and Kyozuka, 2009). OsLAX1 interacts with LAX PANICLE2 (OsLAX2), and both are proposed to act in dependent and independent pathways in AM maintenance (Tabuchi et al., 2011). OsLAX2 regulates tiller and panicle branching in rice during the vegetative and reproductive developmental stages. Similarly, the physical and genetic interactions between *ZmBA1* and *ZmBA2* (orthologs of rice *OsLAX2*) have been shown to regulate AM development in maize. OsLAX2 also regulates grain length by interacting with OsIAA3, thereby interfering with the OsIAA3–OsARF25 interaction involved in the auxin signaling pathway (Zhang et al., 2018).

In barley, grain number per spike is determined mainly by spike rachis node number (SRN), spikelets per node (controlled by row type), and grain number per spikelet. A recent study identified *CCT MOTIF FAMILY 4* (*HvCMF4*) as a regulator of grain number in barley (Huang et al., 2023). Mutations in *HvCMF4* result in higher primordium death rates and pollination failure, which hampers spikelet survival and ultimately leads to a decrease in grain number. Six-rowed spikes can produce more kernels than two-rowed spikes, but they also produce uneven kernels because the kernels on the lateral rows are shorter and thinner than those on the central row (Zwirek et al., 2019). Recently, overexpression of a *CO*-like gene that controls SRN was shown to enhance grain yield in wheat (Zhang et al., 2022). Therefore, generating a higher SRN could be an effective way to increase grain number in barley. However, there have been few studies on the genetic basis of SRN in barley. The availability of high-quality barley reference genomes, especially the release of pan-genomes, has greatly facilitated map-based gene isolation (Mayer et al., 2012; Beier et al., 2016; Jayakodi et al., 2020). Here, we used a recombinant inbred line (RIL) population derived from two Chinese barley cultivars to identify quantitative trait loci (QTLs) for spike traits, including SRN, spike length (SL), and spikelet density (SD). A major QTL for SRN, *qSRN1*, was fine-mapped and cloned. We comprehensively characterized the function of the candidate gene, *HvSRN1*, through CRISPR-Cas9-based gene knockout and analysis of natural variation. Our findings reveal the compound role of *HvSRN1* variation in regulating grain number, kernel size, and weight of barley.

RESULTS

Phenotypic performance of the R90/1815D RIL population

Spike morphological traits, including SRN, SL, and SD, were evaluated in the R90/1815D RIL population and the parental lines across four environments. Both SRN and SL were lower in 1815D than in R90, and 1815D showed a dense spike phenotype with SD ranging from 3.45/cm to 3.54/cm, which was significantly higher ($P < 0.01$) than that of R90 (Figure 1A and Supplemental Table 1). Broad-sense heritability (h^2_B) based on the family mean was high for all three traits (SRN, 97.70%; SL, 98.35%; SD, 98.50%). There was a positive correlation between SRN and SL ($r = 0.46$) and a strong negative correlation between SD and SL ($r = -0.81$) (Supplemental Table 2).

QTL mapping for SRN, SL, and SD

Six QTLs located in four genomic regions were identified for the SRN, SL, and SD traits in the R90/1815D population (Table 1 and Figure 1B), five of which were environmentally stable. The QTL *qSRN1*, on chromosome 2H, was identified as the major stable QTL controlling SRN in the *Y2H5*/*Bmag0378* marker interval (22.6–32.9 cM) and explained up to 37.79% of SRN variation in the combined analysis. *qSL1* (28.2–32.9 cM) overlapped with *qSRN1* and showed a minor effect, explaining 8.20% to 8.94% of SL variation. In barley, *SIX-ROWED SPIKE 1* (*VRS1*), located on chromosome 2HL, plays a crucial role in regulating the fertility of lateral spikelets and determining the spike row type during early spike development (Komatsuda et al., 2007). The *qSRN1* locus was in close proximity to the *VRS1* locus. To ascertain whether *VRS1* was a potential candidate for *qSRN1*, functional markers for *VRS1* were developed and mapped onto the 2H genetic linkage map. QTL analysis revealed no significant effect on SRN at the *VRS1* locus (Figure 1B), indicating that *VRS1* is not the candidate gene for *qSRN1*.

Two additional minor-effect QTLs, *qSRN2* and *qSRN3*, were detected on chromosomes 1H and 4H, respectively. A single QTL

Please cite this article in press as: Fan et al., Natural variations of *HvSRN1* modulate the spike rachis node number in barley, Plant Communications (2023), https://doi.org/10.1016/j.xplc.2023.100670

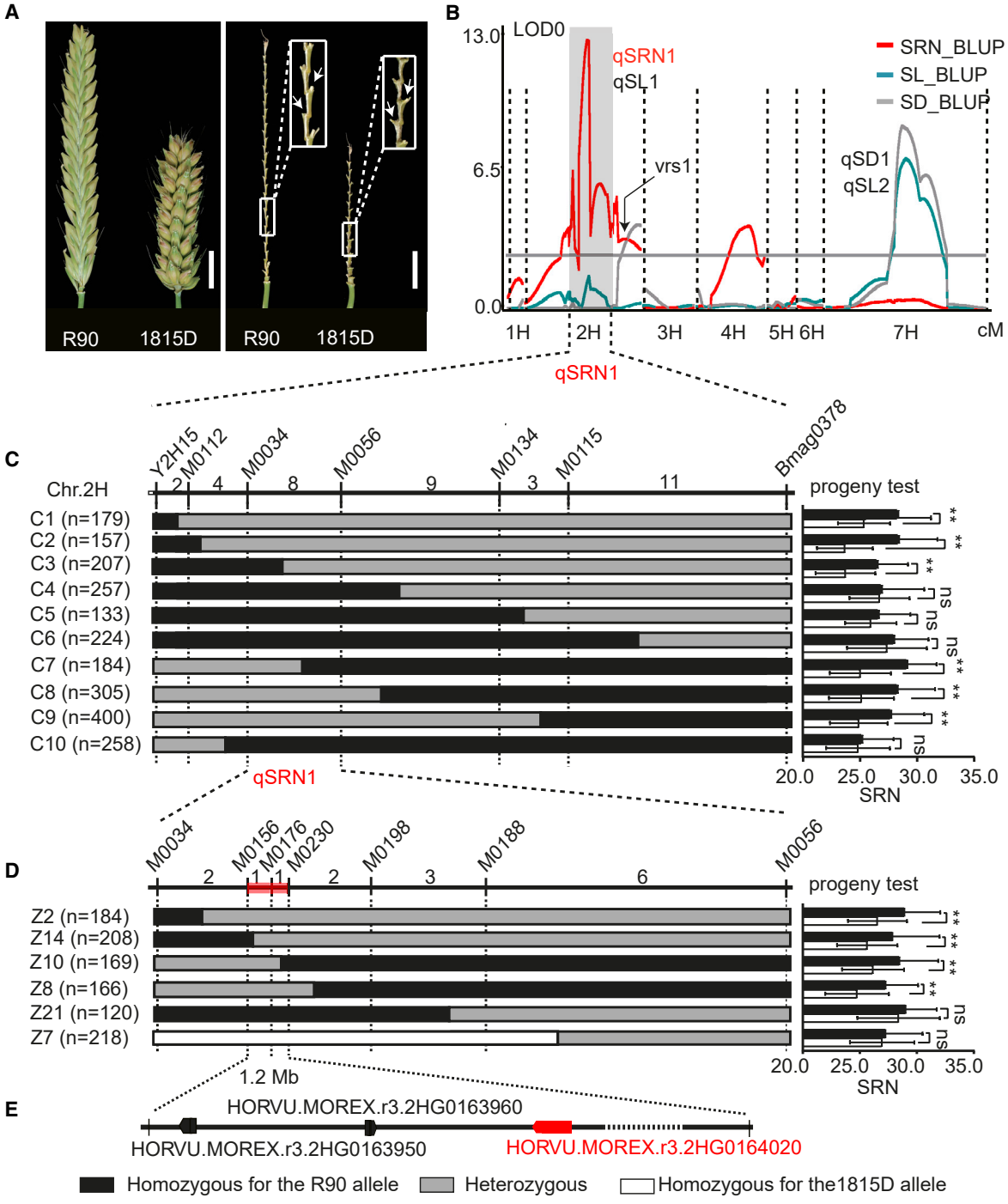

Figure 1. Map-based cloning of *qSRN1*.

(A) Phenotypes of the spike and spike main rachis of R90 and 1815D; white arrows indicate the rachis nodes. Scale bars, 1 cm.

(B) QTL mapping results for SRN, SL, and SD. The arrow indicates the position of the *VRS1* gene.

(C) Fine-mapping of *qSRN1* using F_2 populations (C1–C10) derived from BC_4F_1 recombinants. Left: high-resolution mapping and graphical genotyping of the recombinants. Right: recombinant progeny testing.

(D) Further fine-mapping of *qSRN1* using F_2 populations (Z2, Z14, Z10, Z8, Z21, and Z7) from BC_4F_2 recombinants. Left: high-resolution mapping and graphical genotyping of the recombinants. Right: recombinant progeny testing. Black, gray, and white represent R90, heterozygous, and 1815D alleles, respectively. Significant differences are indicated by $^*P < 0.05$ and $^{**}P < 0.01$. ns indicates no significance (Student's *t*-test).

(E) Three high-confidence genes are predicted to be located in the target region.

Please cite this article in press as: Fan et al., Natural variations of *HvSRN1* modulate the spike rachis node number in barley, Plant Communications (2023), https://doi.org/10.1016/j.xplc.2023.100670

Chromosome	QTL[a]	Pos. (cM)	Nearest marker	LOD	R^2 (%)[b]	Additive[c]	LOD2 interval	Environ.[d]	Physical interval (Mb)[e]
2H	***qSRN1***	31.9	GBM1119	12.56	37.79	−1.87	29.90–32.90	C	151.90–439.94
		24.9	GMS003	27.32	37.27	−2.32	24.20–32.90	E1	
		23.3	Y2H92	18.73	24.56	−1.91	22.60–23.60	E2	
		24.2	GMS003	27.32	37.19	−1.93	23.60–25.40	E3	
		24.2	GMS003	29.5	45.41	−1.82	23.60–25.40	E4	
	qSL1	32.9	GBM1119	5.46	8.94	−0.55	28.20–33.40	E1	
		32.9	GBM1119	4.69	8.2	−0.49	28.20–33.40	E3	
		36.9	bmag0378	5.09	8.58	−0.48	29.10–32.90	E4	
7H	***qSD1***	39.5	Bmac0167	8.53	22.15	0.35	36.90–48.10	C	18.38–582.79
		39.5	Bmac0167	25.4	45.98	0.56	38.00–41.70	E1	
		39.5	Bmac0167	18.79	37.28	0.46	37.70–44.20	E2	
		39.5	Bmac0167	27.05	48.93	0.55	37.80–43.60	E3	
		39.5	Bmac0167	27.3	52.46	0.55	37.90–43.20	E4	
	qSL2	41.5	Bmag0217	7.02	18.69	−0.69	36.50–52.50	C	
		39.5	Bmac0167	23.07	45.31	−1.21	37.70–41.50	E1	
		39.5	Bmac0167	19.47	37.18	−0.95	37.80–41.50	E2	
		39.5	Bmac0167	23.1	45.16	−1.12	37.50–43.60	E3	
		39.5	Bmac0167	22.67	44.87	−1.05	37.50–41.50	E4	
1H	***qSRN2***	1	Bmac0090	3.38	2.9	−0.57	0.00–6.90	E1	180.99–288.52
		1	Bmac0090	4.14	4.29	−0.70	0.00–6.90	E2	
		1	Bmac0090	4.72	3.64	−0.56	0.00–2.30	E3	
		1	Bmac0090	7.44	7.61	−0.72	0.00–2.30	E4	
4H	***qSRN3***	27.1	Ebmag0781	3.88	7.74	−0.85	14.30–34.50	C	411.86–580.93
		27.1	Ebmag0781	9.29	10.7	−1.22	25.70–31.00	E1	
		25.6	Ebmaa0679	5.84	6.62	−0.93	18.30–26.00	E2	
		28.1	Ebmag0781	9.14	9.39	−0.94	22.30–32.30	E3	
		28.1	Ebmag0781	6.15	6.85	−0.73	20.40–33.00	E4	

Table 1. QTLs detected for spike rachis node number, spike length, and spikelet density in the R90/1815D population.

[a]The QTLs shown in bold are environmentally stable.

[b]R^2 is the phenotypic variation explained by the identified QTL.

[c]Positive values represent the additive allele effect from 1815D, whereas negative values are from R90.

[d]C is the combined QTL analysis based on the BLUP across four environments: E1, BJ-2016; E2, BJ-2017; E3, ZJK-2016; and E4, ZJK-2017.

[e]The physical interval was determined using the Morex V3 reference genome.

for SD (*qSD1*) was identified on chromosome 7H and was detected in all environments and in the combined analysis. The likelihood of odd (LOD) and R^2 values for *qSD1* ranged from 8.53 to 27.30 and from 22.15% to 52.46%, respectively. *qSL2*, which controls SL, was identified at the same genetic interval. The LOD value for this QTL ranged from 7.02 to 23.10, and it explained from 18.69% to 45.31% of SL variation (Table 1).

Fine-mapping of *qSRN1*

To fine-map the *qSRN1* locus, we developed a set of new polymorphic markers within the interval of markers *Y2H5* and *Bmag0378*. We identified 10 recombinants from the BC_4F_1 population and generated corresponding F_2 populations for progeny testing (Figure 1C). Markers that exhibited segregation in the F_2 population were selected to genotype the individuals. Specifically, marker *Bmag0378* was selected for the C1–C6 populations, and *M0112* was selected for the C7–C10 populations. Within each F_2 population, plants with different genotypes at the *qSRN1* locus were classified into three groups: R90 homozygous, 1815D homozygous, and heterozygous. We compared differences in average SRN between the two homozygous groups to assess the effect of *qSRN1*. Progeny testing revealed significant differences in SRN between the two homozygous groups in six F_2 populations (C1, C2, C3, C7, C8, and C9). No significant differences were observed in the remaining four populations. These findings suggested that the *qSRN1* locus was located between markers *M0034* and *M0056* (Figure 1C). Average SRN data were significantly higher for the heterozygous group than for the 1815D homozygous group but similar to those of the R90 homozygous group in the six BC_4F_2 populations (Supplemental Figure 1). Next, 16 recombinants, with

Please cite this article in press as: Fan et al., Natural variations of *HvSRN1* modulate the spike rachis node number in barley, Plant Communications (2023), https://doi.org/10.1016/j.xplc.2023.100670

six recombination events, were screened from BC_4F_2 individuals using markers *M0034* and *M0056*. Six recombinant-derived F_2 populations (Z2, Z14, Z10, Z8, Z21, and Z7) were used for further comparative analysis. The progeny test revealed significant differences in SRN between the two homozygous groups in the Z2, Z14, Z10, and Z8 populations but not in Z21 or Z7. Therefore, we finally narrowed down *qSRN1* to the 1.2-Mb physical map interval of *M0156/M0230* (Figure 1D). Three high-confidence candidate genes (*HORVU.MOREX.r3.2HG0163950*, *HORVU.MOREX.r3.2HG0163960*, and *HORVU.MOREX.r3.2HG0164020*) were located in the *qSRN1* mapping interval (Figure 1E).

HvSRN1 is the candidate gene underlying *qSRN1*

Analysis of sequence variation showed that the coding region of *HORVU.MOREX.r3.2HG0164020* contained one synonymous SNP between the two parental lines, and there was no coding sequence variation in the other two genes. Moreover, tissue ePlant viewer showed that only *HORVU.MOREX.r3.2HG0164020* was highly expressed during spike development (Thiel et al., 2021) (Supplemental Figure 2), suggesting its involvement in barley spikelet development. We therefore speculated that *HORVU.MOREX.r3.2HG064020* (*HvSRN1* hereafter) was the potential candidate gene for *qSRN1*.

For further confirmation, we obtained two *HvSRN1* gene knockout mutant lines, *srn1-1* (1-bp insertion) and *srn1-2* (1-bp deletion), through CRISPR-Cas9 targeted editing (Figure 2A). Phenotypic comparison of the wild type and the two homozygous mutants revealed no significant differences in SD. However, SRN and SL were significantly lower in *srn1-1* and *srn1-2* than in wild-type Vlamingh (VL) (Figure 2B–2F). Compared with wild-type VL, *srn1-1* and *srn1-2* also showed significant increases in grain weight, grain length, and grain width of 18.18% and 8.8%, 7.89% and 3.97%, and 6.59% and 3.65%, respectively, but they had lower tiller numbers and seed-setting rates (Figure 2G–2L). These results suggest that *HvSRN1* is responsible for SRN variation and has a pleiotropic effect on grain traits, SL, and tiller number.

Expression patterns of *HvSRN1*

Quantitative real-time PCR (qRT–PCR) revealed that *HvSRN1* was highly expressed in younger spikes and tiller buds (TBs) but barely detectable in roots, leaves, stems, grains, or glumes (Figure 3A). *HvSRN1* expression peaked when the inflorescence reached 1–2 mm (S1–2), the initial stage of spike development from the triple mound to lemma primordia periods, which determine the final SRN (Sreenivasulu and Schnurbusch, 2012; Thiel et al., 2021). *HvSRN1* expression gradually decreased with spike growth stage from stamen primordia to awn primordia (S2–5) and from white anther to green anther (S5–10). Higher expression of *HvSRN1* was observed in R90 at the S1–2 and S2–5 stages, consistent with the higher SRN of R90 and suggesting a strong positive correlation between *HvSRN1* expression and SRN. However, no significant difference in *HvSRN1* expression was observed in TBs of the two parents.

We next performed RNA *in situ* hybridization to investigate the localization of *HvSRN1* expression (Figure 3B). RNA *in situ* hybridization signals demonstrated that the gene was expressed in the early stages of spike development. Specifically, *HvSRN1* transcripts were observed mainly in the spike primordia at the initiation spike primordium stage, indicating involvement of *HvSRN1* in the early initiation of spike development. With spike development, *HvSRN1* was prominently expressed in the IM and spikelet meristem (SM) during the triple mound stage. This suggests that *HvSRN1* plays a crucial role in development of both the inflorescence and spikelet meristems. At the stamen primordia stage, *HvSRN1* expression was observed in the upper SM and IM, further indicating its involvement in spikelet development and floret formation.

To further understand the role of *HvSRN1* in grain number regulation, we analyzed the variation in potential spikelet number and spikelet survival between NIL-*HvSRN1*^{R90} and NIL-*HvSRN1*^{1815D} (Supplemental Figure 3). Potential spikelet number was higher in NIL-*HvSRN1*^{R90} than in NIL-*HvSRN1*^{1815D}, but there was no significant difference in spikelet survival. This suggests that *HvSRN1* primarily regulates grain number by influencing potential spikelet number rather than by affecting spikelet survival.

HvSRN1 protein interacts with HvLAX1 via the RAWUL domain

Protein function annotation indicated that *HvSRN1* encodes a protein of 332 amino acid residues with a RAWUL domain. Phylogenetic analysis was performed based on the conserved amino acid residues, and the proteins were classified into groups I and II (Supplemental Figures 4 and 5). HvSRN1 is the ortholog of OsLAX2 in rice and ZmBA2 in maize. Both groups shared a RAWUL motif at the C terminus of the conserved domain, whereas only group II had a C3HC4-type RING zinc-finger motif at the N terminus. Group I included HvSRN1, OsLAX2, and ZmBA2, which all possess the RAWUL domain responsible for protein–protein interaction (López et al., 2021).

Transient expression in *Nicotiana benthamiana* leaves showed that HvSRN1 is a nuclear-localized protein (Figure 4A). Detection of transcriptional activity revealed the auto-transcriptional activation of full-length HvSRN1 in yeast cells (Figure 4B). Consequently, co-transformation of a series of truncated *HvSRN1* cDNAs with the activation domain (AD)-control revealed that yeast cells with a bait construct encoding a partial *HvSRN1* cDNA of 200–332 amino acid residues failed to grow on selective medium. This construct was then transformed into yeast cells together with an *HvLAX1* cDNA (HORVU3Hr1G087710.1) construct. The transformants grew on the selective medium, indicating a physical interaction between HvSRN1 and HvLAX1. Two truncated *HvSRN1* cDNAs encoding 200–310 and 1–226 amino acid residues were also cloned in bait constructs for analysis of the interaction with HvLAX1. However, no interactions were observed between HvLAX1 and these two constructs. These results suggest that an intact RAWUL domain is responsible for the physical interaction with HvLAX1 (Figure 4B). Firefly luciferase (LUC) complementation imaging analysis was used to confirm the intercellular interactions. Co-expression of *35S*::*HvSRN1-NLuc* with *35S*::*CLuc-HvLAX1* produced strong luciferase activity in *N. benthamiana* leaves (Figure 4C). Overlapping expression regions of *HvSRN1* and *HvLAX1* in both the SM and TB provide compelling evidence for a protein interaction between these two genes (Figure 4D). The

Please cite this article in press as: Fan et al., Natural variations of *HvSRN1* modulate the spike rachis node number in barley, Plant Communications (2023), https://doi.org/10.1016/j.xplc.2023.100670

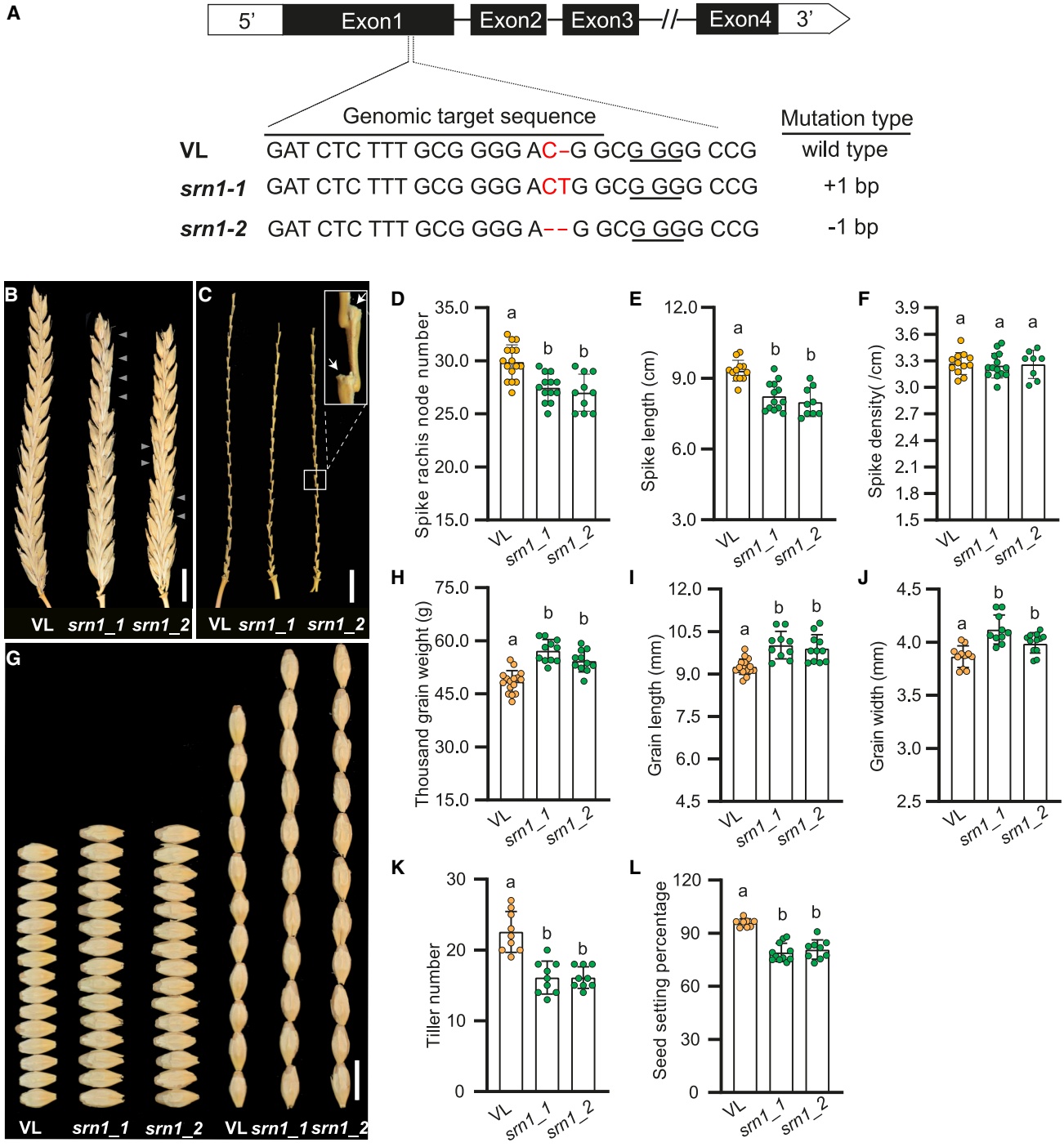

Figure 2. Phenotypic analysis of CRISPR-Cas9-induced *HvSRN1* knockout mutant lines.

(A) Schematic of the gene structure. The target site of the knockout vector is highlighted in red, and the PAM is underlined. "–" represents the deleted nucleotides.

(B and C) Spikes and spike rachis of VL and two mutants. White triangles indicate the sterile spikelets; white arrows indicate the rachis nodes. Scale bars, 1 cm.

(D–F) Comparative analysis of SRN **(D)**, SL **(E)**, and SD **(F)**.

(G) Grains from VL and *srn1-1*/*srn1-2* mutants. Scale bar, 1 cm.

(H–L) Comparative analysis of thousand-grain weight **(H)**, grain length **(I)**, grain width **(J)**, tiller number **(K)**, and seed-setting percentage **(L)**. Data are shown as means ± SD. Bars with the same letter do not differ significantly ($P > 0.01$) based on one-way ANOVA.

Please cite this article in press as: Fan et al., Natural variations of *HvSRN1* modulate the spike rachis node number in barley, Plant Communications (2023), https://doi.org/10.1016/j.xplc.2023.100670

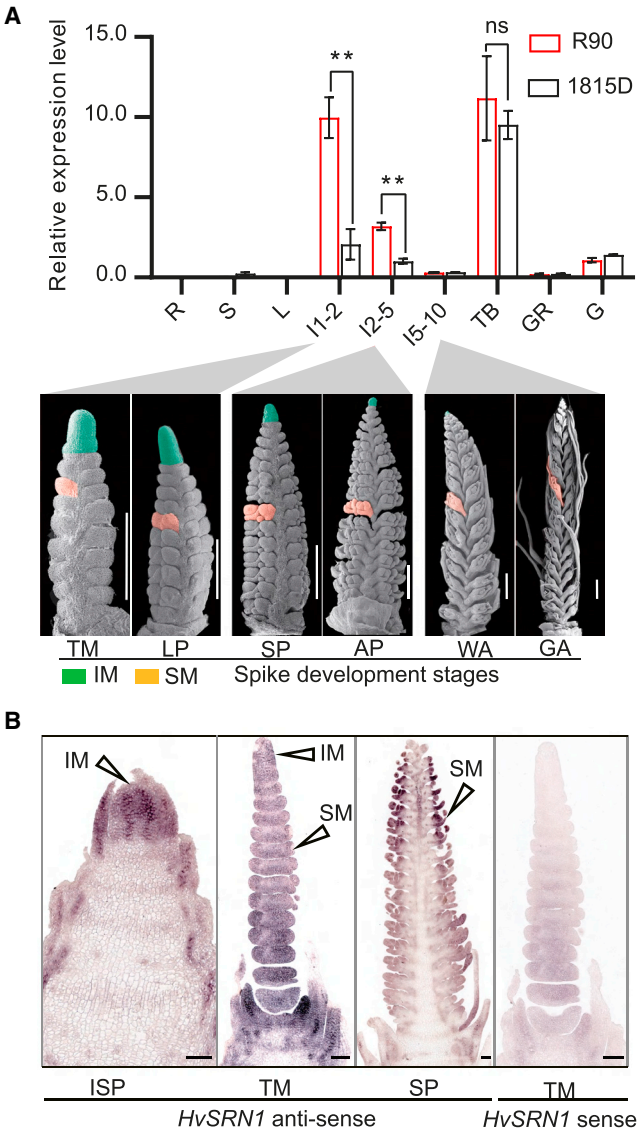

Figure 3. Expression pattern of *HvSRN1*.

(A) Relative expression of *HvSRN1* in various tissues at different growth stages. Expression levels in roots (R), stems (S), leaves (L), young spikes of 1–2 mm (S1–2), 2–5 mm (S2–5), and 5–10 mm (S5–10), tiller buds (TB), grain glumes (GR), and grain (G) (10 days after pollination) are shown. Data are presented as means ± SD. n = 3. Significant differences are indicated by $^{**}P < 0.01$ (Student's *t*-test). ns, not significant. The panels show corresponding scanning electron microscope images of spike developmental stages from the triple mound stage to the green anther stage. TM, triple mound; LP, lemma primordia; SP, stamen primordia; AP, awn primordia; WA, white anther; GA, green anther; IM, inflorescence meristem; SM, spikelet meristem. Scale bars, 500 μm.

(B) *In situ* hybridization of *HvSRN1*. Longitudinal sections of spike developmental stages from the initiation spike primordium stage (ISP) to the SP stage. Scale bars, 100 μm.

spatial distributions of *HvSRN1* and *HvLAX1* showed some inconsistencies, with a notable lack of *HvLAX1* transcripts in the IM.

HvSRN1 haplotype and promoter activity analysis

The R90/1815D parental lines showed one synonymous substitution in the *HvSRN1* coding region and four InDels and four SNPs in the promoter region (Figure 5A). On the basis of the nucleotide polymorphisms in the promoter region, we divided the sequences of 389 global barley accessions into 12 haplotypes (Figure 5B and Supplemental Table 3). Phylogenetic analysis classified the 12 haplotypes into two groups—four haplotypes (Haps 1, 2, 3, and 4) in group I (*HvSRN1*^{R90} allele) and eight in group II (*HvSRN1*^{1815D} allele) (Figure 5C). Multiple comparisons of average SRN data of the accessions collected from three environments showed no significant differences among the haplotypes within either of the groups. However, haplotypes in group I, with three consensus SNPs (SNP-1884, SNP-1748, and SNP-1699), exhibited a higher average SRN than those in group II (Figure 5B).

To determine the effects of these three SNPs, we transiently expressed site-directed mutated promoter fragments of *HvSRN1* (Figure 5D). The relative LUC/REN values of SNP-1884 or/and SNP-1748 mutations were significantly lower than those of the *HvSRN1*^{R90} promoter and were comparable to those of the 1815D promoter. Moreover, the SNP-1699 mutation did not significantly alter promoter activity compared with R90. We concluded that the group I haplotypes, with three consensus SNPs in the promoter region, represented the high-SRN haplotype. SNP-1884 and SNP-1748 were inferred to be the functional nucleotide polymorphisms (FNPs) accounting for the variation in *HvSRN1* expression between R90 and 1815D. However, analysis with the PLACE tool revealed no well-known *cis*-regulatory elements at these two sites (Higo et al., 1999).

These two FNPs constitute the "CAG" and "CG" sequence context in 1815D, where cytosine residues could be methylated. We therefore examined the methylation level of the promoter segment (from −1950 to −1644 bp) containing these two functional sites in young spikes. The two sites were highly methylated in 1815D (SNP-1884, 72.72%; SNP-1748, 100%), but no methylation was detected in R90 (SNP-1884, 0.0%; SNP-1748, 0.0%) (Supplemental Figure 6). This could explain the lower expression of *HvSRN1* in 1815D than in R90.

Evolution and distribution of *HvSRN1*

Haplotype analysis showed that 10 wild barley (*Hordeum spontaneum* L.) accessions shared the same haplotypes with Hap 3 but not with Hap 9, suggesting that Hap 3 was derived directly from wild barley. Network analysis revealed that Haps 1, 2, and 4 were closely related to Hap 3, suggesting that these haplotypes may have originated from Hap 3 (Figure 5E). Hap 12, comprising both wild barley and landraces, was genetically close to Hap 6, Hap 8, Hap 9, Hap 10, and Hap 11, suggesting that these haplotypes might have originated from Hap 12. Wild barley in Hap 3 showed a large genetic distance from that in Hap 12, indicating that Hap 3 and Hap 9 of domesticated barley have independent origins.

The geographic distribution of the two FNPs revealed clear geographic divergence between the high (*HvSRN1*^{R90}) and low (*HvSRN1*^{1815D}) SRN alleles (Figure 5F). The *HvSRN1*^{R90} allele was widely distributed in Europe, Northeast Africa, and East Asia. The *HvSRN1*^{1815D} allele was distributed mainly in South-Central Asia, the Qinghai-Tibet Plateau, and other higher-altitude regions. About 70.1% of the cultivars contained the *HvSRN1*^{R90}

Please cite this article in press as: Fan et al., Natural variations of *HvSRN1* modulate the spike rachis node number in barley, Plant Communications (2023), https://doi.org/10.1016/j.xplc.2023.100670

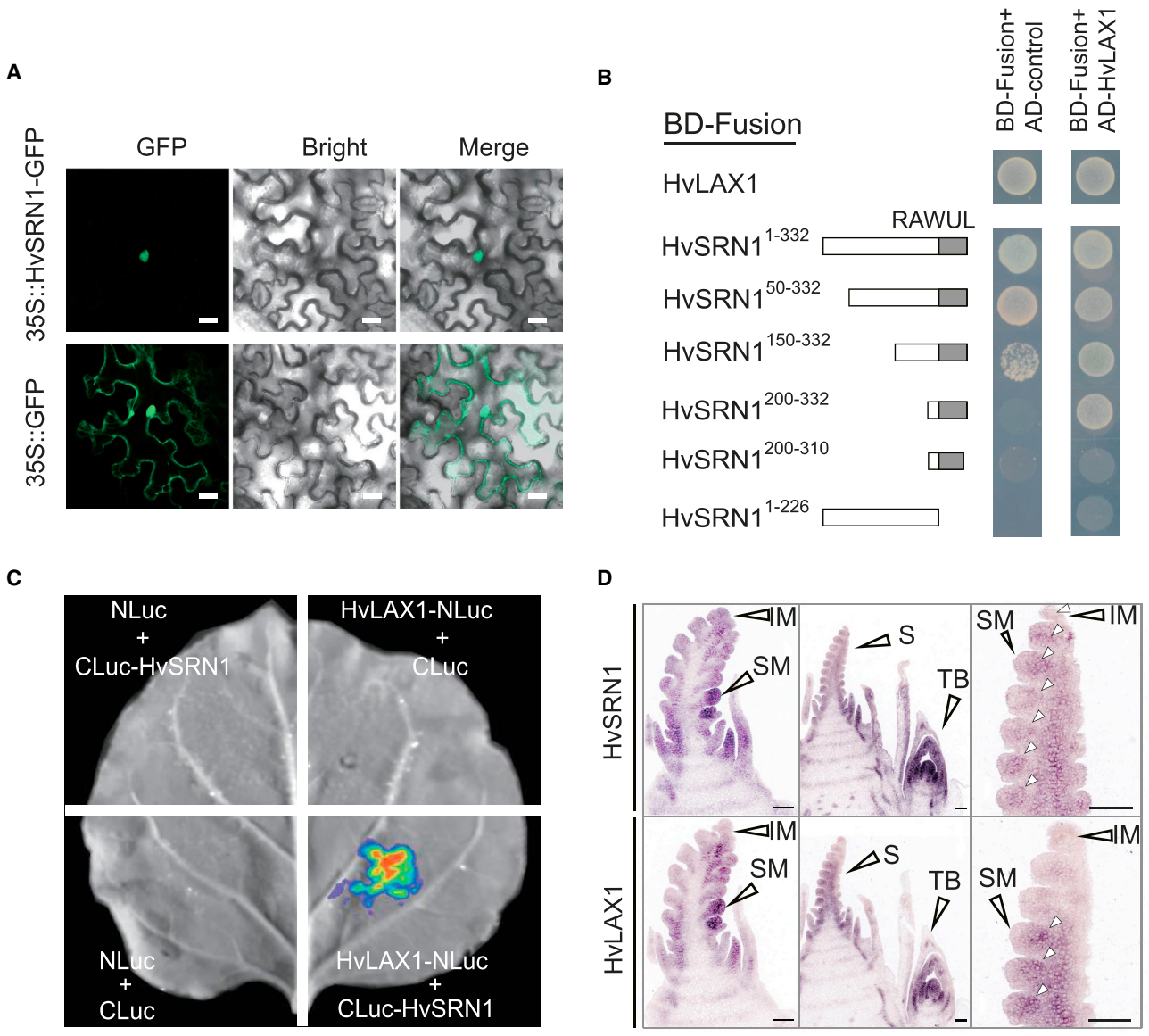

Figure 4. Characterization of the *HvSRN1* gene and its encoded protein.

(A) Subcellular localization of *ProSuper*::*GFP* and *ProSuper*::*HvSRN1-GFP* in tobacco leaf cells. Scale bars, 20 μm.

(B) Interactions between HvSRN1 and HvLAX1 were tested using a yeast two-hybrid assay. The full-length *HvLAX1* and *HvSRN1* genes, as well as a series of truncated *HvSRN1* genes, were fused with a DNA binding-domain construct (BD), and full-length *HvLAX1* was fused with an activation domain construct (AD). Yeast cells were grown on TDO (SD–His/-Leu/-Trp) medium. The gray box represents the position of the RAWUL domain.

(C) Firefly luciferase complementation imaging assays in *Nicotiana benthamiana* leaves confirm the HvSRN1–HvLAX1 interaction. N- and C-terminal fragments of luciferase (LUC) were fused with the indicated proteins, and the indicated pairs were co-expressed in *N. benthamiana* leaves. CLuc-HvSRN1/empty-nLuc, HvLAX1-nLuc/CLuc-empty, and empty-nLuc/CLuc-empty vectors were used as negative controls.

(D) *In situ* hybridization of *HvSRN1* and *HvLAX1* mRNA expression in longitudinal sections of the young spike. Scale bars, 100 μm.

allele, whereas only 29.9% contained the $HvSRN1^{1815D}$ allele. Intriguingly, 93.75% of the $HvSRN1^{R90}$ allele was found in two-rowed barley, whereas the $HvSRN1^{1815D}$ allele (62.44%) was mainly found in six-rowed cultivars (Supplemental Table 4).

HvSRN1^{R90} increases the grain yield of barley

We next compared the yield-related traits of NIL-$HvSRN1^{R90}$ and NIL-$HvSRN1^{1815D}$ under field conditions. Compared with NIL-$HvSRN1^{1815D}$, NIL-$HvSRN1^{R90}$ showed average increases of 49.9 in grain number and 1.46 g in grain yield increase per plant; it had significantly higher SRN and SL but lower grain weight/size (Figure 6A–6M). However, the tiller number and SD of NIL-$HvSRN1^{1815D}$ were comparable to those of NIL-$HvSRN1^{R90}$ (Figure 6N and 6O). Although some samples were temporarily transplanted into pots (Figure 6A and 6B) to visually assess overall plant morphology, the yield-related trait analysis itself was performed under field conditions to ensure accuracy and reliability.

Analysis of *HvSRN1* expression revealed a clear disparity between young spikes of NIL-$HvSRN1^{1815D}$ and those of

Please cite this article in press as: Fan et al., Natural variations of *HvSRN1* modulate the spike rachis node number in barley, Plant Communications (2023), https://doi.org/10.1016/j.xplc.2023.100670

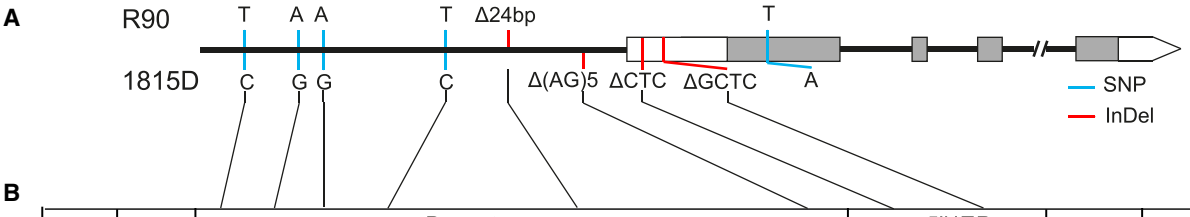

B

	Hap.	Promoter -1884	-1748	-1699	-1162	-851	-429	5'UTR -276	-200	No.of cv.	SRN
Group I	Hap 1	T	A	A	T	AGTGATCTAAACGTTTTTATAT	(AG)5	CTC	GCTC	19	22.97 a
	Hap 2	T	A	A	T	-	(AG)5	-	-	11	22.22 a
	Hap 3	T	A	A	T	-	(AG)5	CTC	GCTC	214	21.95 a
	Hap 4	T	A	A	C	-	(AG)5	CTC	GCTC	17	21.72 a
Group II	Hap 5	C	G	G	T	-	(AG)5	(CTC)2	TCGCTC	12	19.98 b
	Hap 6	C	G	G	C	-	-	-	-	30	19.85 b
	Hap 7	C	G	G	T	-	(AG)5	CTC	GCTC	22	19.80 b
	Hap 8	C	G	G	C	-	-	CTC	GCTC	9	19.49 b
	Hap 9	C	G	G	C	AGTGATCTAAACGTTTTTATAT	-	-	-	40	19.37 b
	Hap 10	C	G	G	T	-	-	-	-	5	18.84 b
	Hap 11	C	G	G	T	AGTGATCTAAACGTTTTTATAT	-	-	-	8	18.38 b
	Hap 12	C	G	G	C	AGTGATCTAAACGTTTTTATAT	-	CTC	GCTC	2	-
Wild	-	T/C	A/G	A/G	T/C	AGTGATCTAAACGTTTTTATAT/-	(AG)n	(CTC)n	(GCTC)n	56	-

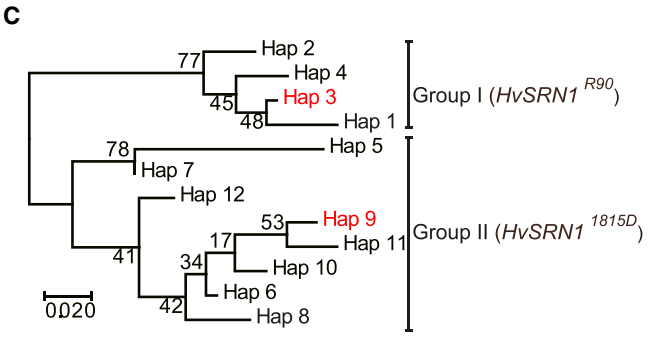

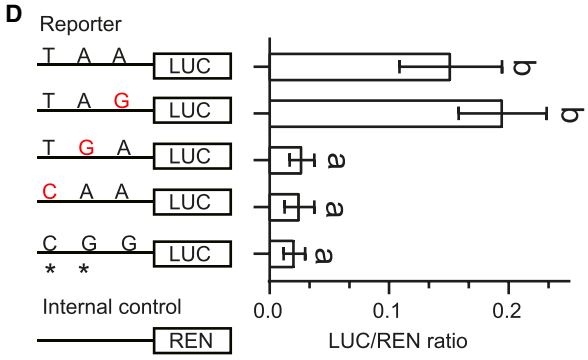

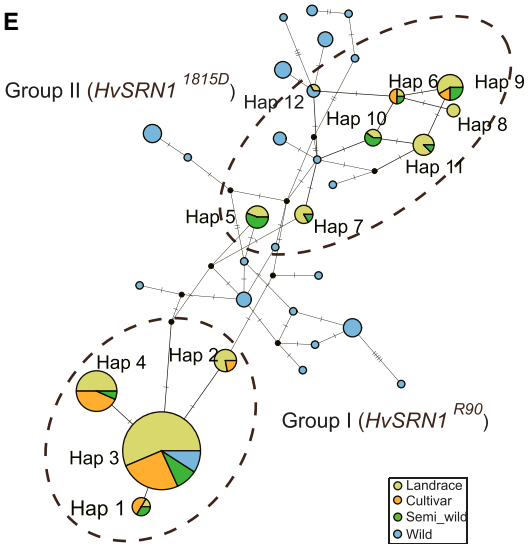

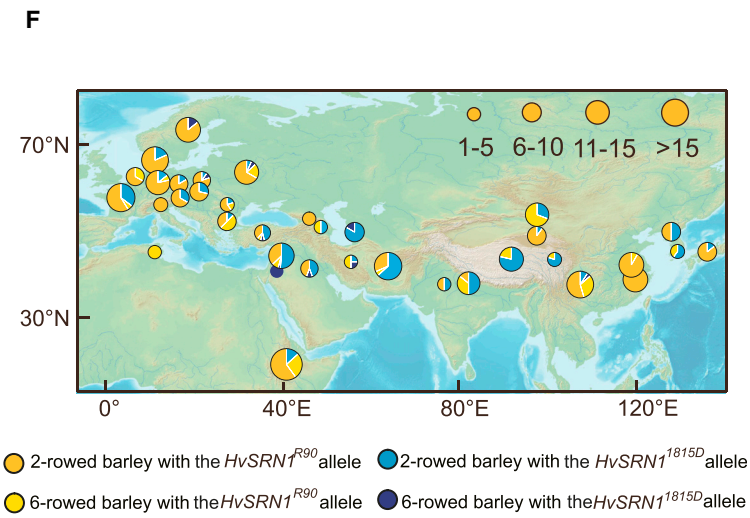

Figure 5. Haplotype analysis of *HvSRN1*.

(A) Schematic of gene structure; allelic variations in *HvSRN1* between R90 and 1815D are indicated by vertical lines at the bottom.

(B) Haplotype analysis of the *HvSRN1* promoter region from 389 barley accessions. SRN data for each barley accession were collected in three different environments. Values that share a lowercase letter do not differ significantly ($P > 0.01$) according to one-way ANOVA.

(legend continued on next page)

Please cite this article in press as: Fan et al., Natural variations of *HvSRN1* modulate the spike rachis node number in barley, Plant Communications (2023), https://doi.org/10.1016/j.xplc.2023.100670

NIL-*HvSRN1*^{R90} (Supplemental Figure 7). However, no significant difference in expression was observed in TBs. These findings suggest that the expression level of *HvSRN1* plays an important role in regulating inflorescence development and grain number per spike. However, it remains to be determined whether *HvSRN1* has any effect on tiller formation at the transcriptional level.

DISCUSSION

Pleiotropy or tight linkage of colocalized QTLs for spike morphological traits on chromosomes 2H and 7H

Spike morphological traits, including SRN, SL, and SD, affect grain yield and quality in barley (Zhai et al., 2016; Hagenblad et al., 2019). The SRN, SL, and SD of these genotypes showed consistent variation across four environments. Variations in SRN, SL, and SD could be stably inherited across different environments. Increased grain number always manifests as an increase in SRN and/or spikelets per node in barley. In general, six-rowed barley has a higher grain number than two-rowed barley. This difference in grain number is mainly attributed to the influence of *VRS1–5* genes, which play a crucial role in determining barley row type by affecting the fertility and size of lateral spikelets (Zwirek et al., 2019). These *VRS* genes inhibit fertility during emergence of carpels and awns in developing lateral spikelets. At present, there are no reports demonstrating that *VRS* directly regulates SRN. Therefore, we selected SRN instead of grain number per spike as the target trait, which effectively eliminated the effect of row type in the R90/1815D population. Furthermore, the physical intervals of the QTLs identified in our study did not contain any *VRS* genes. For instance, *VRS2* and *VRS4* genes are located on chromosomes 5H and 3H, respectively (Koppolu et al., 2013; Youssef et al., 2017), but we did not detect any QTLs related to the three morphological traits on these chromosomes. Similarly, *VRS3* was located at 358.25 Mb on chromosome 1H (van Esse et al., 2017), which was outside the physical range (180–288 Mb) of *qSRN1* identified in the R90/1815D population. In addition, *VRS5* is located at 15.84 Mb on chromosome 4H (de Souza Moraes et al., 2022), inconsistent with the physical location of *qSRN3* (411.86–580.93 Mb) detected in the R90/1815D population.

We identified two major genomic regions controlling spike morphological traits in the R90/1815D population—one on 2H (*qSL1* and *qSRN1*) and one on 7H (*qSL2* and *qSD1*)—each of which contained two loci. These colocalizations may be due to pleiotropy or tight linkage between genes that govern the traits (Chebib and Guillaume, 2021). Dissection and cloning of the 2H region revealed that *HvSRN1* controls SRN and has a pleiotropic effect on SL. To date, several loci that affect SD in barley have been reported, including dense *spike-ar* (*dsp.ar*) and *Zeo* (*ZEOCRITON1*) (Shahinnia et al., 2012). The locus *dsp.ar* was mapped to the centromere of chromosome 7H, and it may share a similar genomic region with the colocalized QTL for SD (*qSD2*) and SL (*qSL2*) identified in our study. Here, we found that SD was strongly negatively correlated with SL but not significantly correlated with SRN, indicating that SL largely determines SD. We therefore inferred that the candidate genes in the chromosome 7H region might pleiotropically control SD and SL.

Conservation and diversification of *HvSRN1*/*OsLAX2*/*ZmBA2* functions in barley, rice, and maize

The homologs *HvSRN1*, *OsLAX2*, and *ZmBA2* exhibit similar expression patterns and encode proteins that physically interact with HvLAX1/OsLAX1/ZmBA1 to regulate SRN, indicating that the *LAX* genes are evolutionarily conserved across different cereal crops. In addition, a trade-off between grain number and grain size was found in both *srn1-1* and *Oslax2* mutants (Tabuchi et al., 2011; Zhang et al., 2018). Unlike that of maize BA1, the interaction of HvSRN1 and HvLAX1 may have the same function as the OsLAX2–OsLAX1 module in regulation of tiller numbers during the vegetative stages. We also observed some differences in phenotypic trait values. In rice, the number of spikelets was more than 50% lower in the *Oslax2* mutant than in the wild type (Tabuchi et al., 2011). Likewise, the number of maize tassel branches and spikelets was reduced by more than 50% in the *Zmba2* mutant (Yao et al., 2019). However, *srn1-1* showed only a 10% decrease in SRN. This difference in phenotype may be attributed to differences in spike architecture among the three crops. Unlike barley, which has an unbranched spike inflorescence, rice and maize have branched inflorescences with well-defined secondary branches. These distinct cereal inflorescence structures may restrict the potential of the *LAX* family. The *srn1* mutant exhibited sterile spikelets, and expression profiling of *HvSRN1* shed light on its regulatory role in barley floral development. By contrast, the analogous *Oslax2* mutant in rice has not yielded comparable observations (Tabuchi et al., 2011; Zhang et al., 2018). This incongruity could plausibly be ascribed to differences in spike architecture between the two crops, which may engender distinct phenotypic manifestations. Further studies are needed to determine the molecular basis for these differences and their potential implications for crop improvement.

In recent decades, studies have advanced our understanding of the genetic basis of inflorescence development. Numerous genes that control grain number have been isolated using positional cloning methods. All these efforts were based on characterization of classical mutants or natural variations. Owing to the extreme phenotype of the mutants, their genetic mutations are always eliminated during the selection process. However, natural variations in crop varieties with moderate phenotypic changes persist over several years; these variants respond to long-term natural and artificial selection and have led to the

(C) Phylogenetic tree of the 12 haplotypes.
(D) Transient expression assay of promoter activity; n = 5. Left: constructs with site-directed mutations at the three SNPs in the promoter region. Right: relative LUC/REN values. Error bars denote SDs. Bars that share a lowercase letter do not differ significantly ($P > 0.01$) according to one-way ANOVA.
(E) Haplotype network of *HvSRN1*. Two different haplotype groups are circled with dashed ellipses.
(F) Geographic distribution and allele frequencies of 525 barley cultivars. Cultivars were assigned to their source country. Orange circle: two-rowed barley with the *HvSRN1*^{R90} allele; yellow circle: six-rowed barley with the *HvSRN1*^{R90} allele; blue circle: two-rowed barley with the *HvSRN1*^{1815D} allele; sky-blue circle: six-rowed barley with the *HvSRN1*^{1815D} allele.

Please cite this article in press as: Fan et al., Natural variations of *HvSRN1* modulate the spike rachis node number in barley, Plant Communications (2023), https://doi.org/10.1016/j.xplc.2023.100670

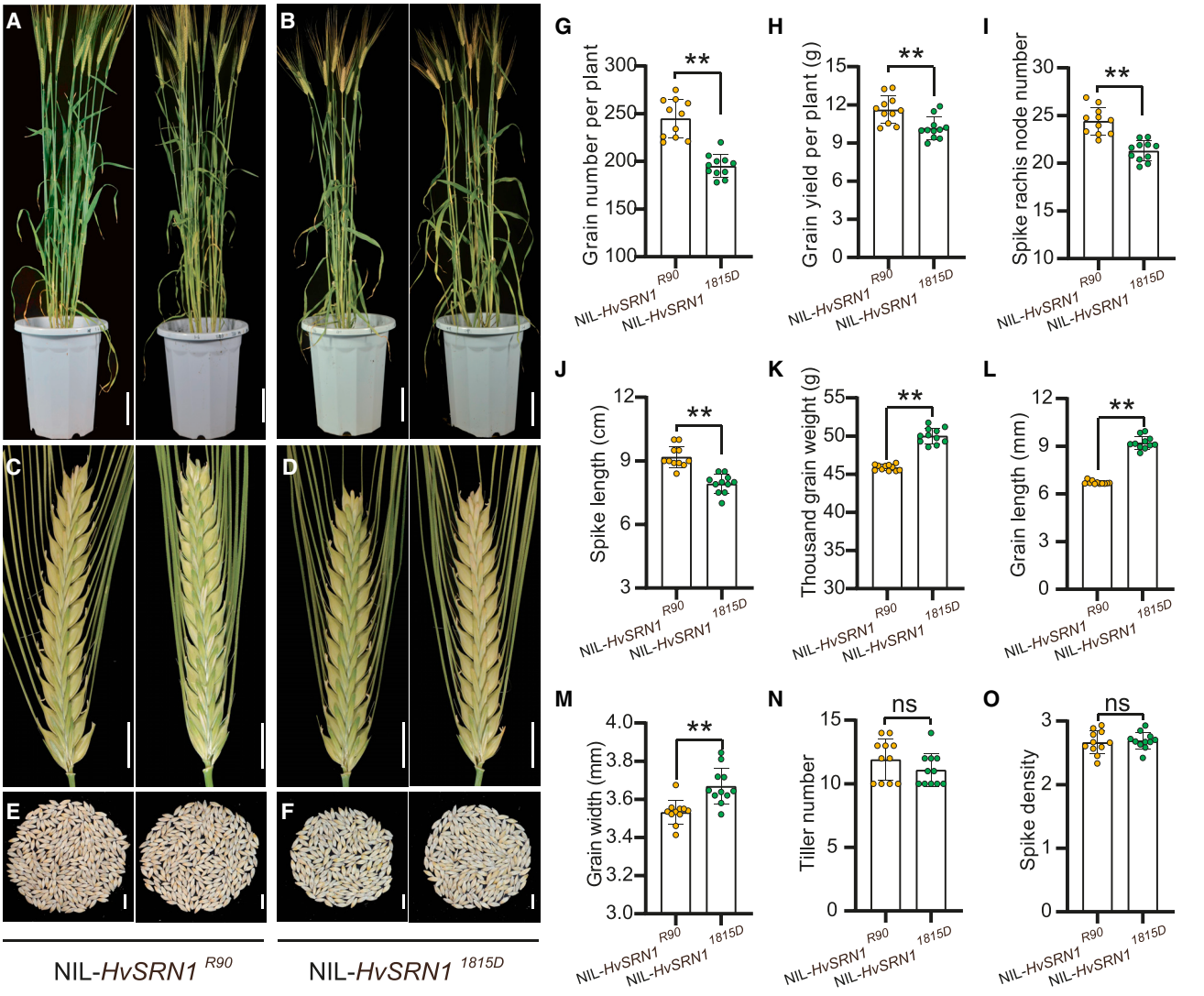

Figure 6. *HvSRN1*^{R90} increases the total grain yield per plant.

(A and B) Plant appearance. Scale bars, 10 cm.

(C and D) NIL-*HvSRN1*^{R90} and NIL-*HvSRN1*^{1815D} spikes. Scale bars, 1 cm.

(E and F) Total grains per plant of NIL-*HvSRN1*^{R90} and NIL-*HvSRN1*^{1815D}. Scale bars, 10 cm.

(G–O) Grain number per plant **(G)**, grain yield per plant **(H)**, spike rachis node number **(I)**, spike length **(J)**, thousand-grain weight **(K)**, grain length **(L)**, grain width **(M)**, spikelet density **(N)**, and tiller number **(O)** of NIL-*HvSRN1*^{R90} and NIL-*HvSRN1*^{1815D}. Values are the means ± SD. *P* values were calculated using Student's *t*-test. $^{**}P < 0.01$; ns, not significant.

development of phenotypes (Liang et al., 2021). In our study, *HvSRN1* was detected by a map-based strategy using a bi-parental mapping population, and different frequencies of two *HvSRN1* alleles were found in two- and six-row barley panels. These results support the notion that regulation of grain number by *HvSRN1* may have been under selection during barley domestication. By contrast, cloning of *OsLAX2* and *ZmBA2* was based on mutants. Therefore, it is unclear whether these genes have been under selection, and fine-tuning these genes in rice or maize could be effective for improving yield potential.

Domestication of *HvSRN1* and its potential value in barley breeding

Several studies have shown that the physiological mechanism underlying the trade-off between grain number and grain size is the competition for photoassimilates (Fischer, 2011). However, little is known about the underlying genetic basis of this phenomenon. The rice GSN1–MAPK module has been shown to coordinate the trade-off between grain number and size by integrating localized cell differentiation and proliferation (Guo et al., 2018). Interestingly, a previous study reported that *OsLAX2/Gnp4* is expressed in glumes and participates in the OsIAA3–OsARF25–OsERF142 pathway to regulate grain length and size (Zhang et al., 2018). Here, *HvSRN1* also appeared to affect the trade-off between grain number and grain size. However, it was barely expressed in barley glumes, suggesting that *HvSRN1* might participate in other pathways to regulate grain size in barley.

Many efforts have been made to overcome or balance the trade-off between grain number and size to improve grain yield

Please cite this article in press as: Fan et al., Natural variations of *HvSRN1* modulate the spike rachis node number in barley, Plant Communications (2023), https://doi.org/10.1016/j.xplc.2023.100670

potential. Ectopic expression of *TaExpA6* in early-developing wheat seeds increased grain weight without negatively affecting grain number. It ultimately increased grain yield by almost 11.3%, overcoming the common bottleneck to yield improvement in wheat (Calderini et al., 2021). In rice, a copy-number variation in the upstream region of *FZP*, consisting of an 18-bp DNA fragment, fine-tuned *FZP* expression during panicle branching, resulting in a substantial increase in grain number and a slight decrease in kernel weight and ultimately increasing rice grain yield by more than 15% (Bai et al., 2017). In the present study, NIL-*HvSRN1*^{R90} had a significantly higher grain yield per plant compared with NIL-*HvSRN1*^{1815D} in two-rowed barley, indicating that higher expression of *HvSRN1* could coordinate the trade-off between grain number and grain size. These results suggest that the two FNPs in the *HvSRN1* promoter can regulate *HvSRN1* expression and affect grain number, and they could therefore be utilized in barley breeding.

To increase grain number, ancient farmers selected six-rowed barley derived from two-rowed wild barley that contained a point mutation of a dominant allele at the *VRS1* locus (Komatsuda et al., 2007). This mutation probably originated in the western Mediterranean, approximately 7000–6000 years BP, and spread rapidly throughout the western cultivation range of barley (Tanno et al., 2002). The mutation of row-type genes led to a six-rowed phenotype with a significant increase in grain number during barley domestication. Owing to the different end uses and breeding objectives of two-rowed and six-rowed barley, their improvement has been carried out independently (Wang et al., 2015). For instance, in two-rowed barley, the grain number per spike depends largely on potential spikelet number, whereas in six-rowed barley, it depends mainly on spikelet survival ability (Thirulogachandar et al., 2021). In our study, *HvSRN1* was found to influence grain number by regulating potential spikelet number, similar to the manner in which grain production is enhanced in two-rowed barley. In addition, we found that the high-SRN allele *HvSRN1*^{R90} was dominant in two-rowed barley—indeed, the wide distribution of the *HvSRN1*^{R90} allele might be attributed to its ability to enhance yield potential in two-rowed barley—whereas only a small proportion of *HvSRN1*^{R90} was found in six-rowed barley. Consequently, we speculate that the potential for *HvSRN1* to enhance grain number by promoting potential spikelet number may have been weakened during the selection and domestication process of six-rowed barley, potentially owing to the impact of row-type genes.

Because *HvSRN1* plays a critical role in SRN and SL regulation, it affects the trade-off between grain number and size. We propose that the *HvSRN1*^{R90} allele was preferentially selected in two-rowed barley to increase SL and grain number, whereas the *HvSRN1*^{1815D} allele was chosen to promote grain size in six-rowed barley. Introgression of *HvSRN1*^{R90} into six-rowed barley with high grain size may be valuable for breeding of high-yielding barley cultivars. Intriguingly, we found that the *HvSRN1*^{1815D} allele was prevalent in several high-altitude areas characterized by harsh environmental conditions, possibly because of the superior adaptability of six-rowed barley (Comadran et al., 2012; Wang et al., 2015). In general, six-rowed barley tends to have a shorter growth season. The *HvSRN1*^{1815D} allele, with low SRN, requires fewer nutrient resources compared with the *HvSRN1*^{R90} allele, allowing the plant to spike earlier in the shorter growing season. Overall, our findings demonstrate the importance of *HvSRN1* in barley breeding and its role in the regulation of grain development.

METHODS

Plant materials and field experiments

An RIL population, comprising 145 lines derived from a cross between 1815D and R90, was used to identify QTLs underlying SRN, SL, and SD. Field experiments were carried out in Beijing (BJ) and ZhangJiaKou, HeBei (ZJK) in China during two growing seasons (2016 and 2017). Data were obtained from four environments (BJ-2016 [E1], BJ-2017 [E2], ZJK-2016 [E3], and ZJK-2017 [E4]).

For NIL development, one RIL line (RIL26) was crossed with the recurrent parent (R90). The resulting progeny underwent four generations of backcrossing with the recurrent parent to produce the BC_4 generation. In each generation, a marker-assisted selection strategy was used to perform both foreground and background selection. A total of 574 BC_4F_1 individuals were produced for subsequent analyses. First, 10 recombinants (BC_4F_1) within the *qSRN1* region were selected to produce the corresponding F_2 populations (BJ-2018). Next, over 50 individuals that exhibited heterozygosity at the QTL region were self-pollinated to produce BC_4F_2 populations, which were used to screen for recombinants (BJ-2018). Eight BC_4F_1 individuals were then backcrossed with R90 to produce BC_5F_1 plants. Homozygous lines (BC_5F_3) such as NIL-*HvSRN1*^{R90} and NIL-*HvSRN1*^{1815D} were selected for further analysis. To further delimit *qSRN1*, six recombinants were selected from the BC_4F_2 populations, and their corresponding F_2 populations were evaluated (BJ-2019).

To evaluate the effect of different haplotypes on SRN, we analyzed 389 barley accessions (146 from the IPK_Genebank core set; 243 from the Chinese_Genebank core set). These materials were planted and cultivated in three environments: BJ-2018, BJ-2019, and ZJK-2019. To determine the geographic distribution of the two *HvSRN1* alleles, 525 barley cultivars collected from across the world were used for genetic diversity analyses. To ensure accurate data, other materials such as VL, *srn_1*, *srn_2*, NIL-*HvSRN1*^{R90}, and NIL-*HvSRN1*^{1815D} were planted in 15 replicates. Each replicate consisted of a single row.

Phenotypic analysis

The main spikes of 10 plants from the RIL population, 389 barley accessions, and transgenic materials were randomly selected for phenotype analysis. SRN was counted from the base rachis node to the top rachis node. SL was measured from the base rachis node to the topmost rachis node. SD was defined as the ratio between SRN and SL. Mature grains of transgenic materials were harvested and bulked for each replicate, and thousand-grain weight, grain length, and grain width were determined using a camera-assisted phenotyping system (Wanshen SC-G seed detector, Hangzhou Wanshen Detection Technology, Hangzhou, China). Phenotype analysis of recombinant-derived F_2 populations and two NILs (NIL-*HvSRN1*^{R90} and NIL-*HvSRN1*^{1815D}) was performed on a single-plant basis. Mature grains per plant of the two NILs were collected and phenotyped using the camera-assisted phenotyping system. Potential spikelet number was determined using the method described by Thirulogachandar and Schnurbusch (2021). Final spikelet number of the main spike was counted after harvesting. Spikelet survival was calculated by dividing the final spikelet number by the potential spikelet number. Three randomly selected plants for each replicate were used to phenotype the two NILs for each trait.

The best linear unbiased prediction (BLUP) of the three traits and the h^2_B of SRN, SL, and SD were calculated using SAS version 9.1 (SAS Institute, Cary, NC, USA). IBM SPSS 27 (IBM SPSS, Armonk, NY, USA) was used for Pearson's correlation analysis of phenotypic data and BLUP values

Please cite this article in press as: Fan et al., Natural variations of *HvSRN1* modulate the spike rachis node number in barley, Plant Communications (2023), https://doi.org/10.1016/j.xplc.2023.100670

to assess the relationships among the three spike morphological traits. Significant differences were evaluated using Student's *t*-test.

Linkage and QTL analysis

Seventy-one polymorphic SSR markers (mostly obtained from http://wheat.pw.usda.gov/GG3/) were used to genotype the RIL population. The genetic linkage map was constructed using JoinMap 4.0 with an LOD value of 10 (van Ooijen, 2006). WinQTLCart2.5 software was used to identify QTLs using the composite interval mapping method.

Fine mapping of *qSRN1* and cloning the genomic DNA of *HvSRN1*

Markers flanking the QTL were used to define the target region, which was compared with the reference genome sequence of barley cv. Morex V3 (https://edal.ipk-gatersleben.de/). SSR and InDel markers were developed using Primer3 software (https://bioinfo.ut.ee/primer3-0.4.0/). Genomic DNA of candidate genes amplified from 1815D and R90 was sequenced and analyzed. The markers used for QTL positional cloning are listed in Supplemental Table 5.

CRISPR-Cas9-mediated mutation of *HvSRN1*

To prepare the CRISPR-Cas9 (*HvSRN1*) construct, a 20-bp DNA sequence with an NGG (protospacer adjacent motif [PAM]) at the 3′ end of the first exon of *HvSRN1* was designed using E-CRISP Design (http://www.e-crisp.org/E-CRISP/). This sequence was inserted into the plant binary vector as described previously (Ma et al., 2015). The expression vectors were introduced into *Agrobacterium* strain C58C1 using a triparental mating strategy (Ditta et al., 1980). Barley transformation was performed as described by Wang et al. (2017). Immature embryos isolated from pollinated barley cv. Vlamingh (VL) were used for *Agrobacterium*-mediated transformation.

RNA extraction, cDNA preparation, and qRT–PCR

Total RNA was extracted from various plant tissues using TRIzol reagent (Invitrogen). Total RNA was used to synthesize first-strand cDNA with a PrimeScript II 1st Strand cDNA synthesis kit (Vazyme). R90 and 1815D samples were isolated and analyzed during the vegetative and reproductive stages; they included samples of young leaves, roots, stems, grain, grain glumes, and various younger spike stages. qRT–PCR was performed on an ABI7500 instrument using SYBR Green PCR Master Mix. At least three biological replicates were performed for all experiments. The barley actin gene (*HORVU.MOREX.r3.1HG0003140.1*) was used as an internal reference gene.

RNA *in situ* hybridization

In situ hybridization was performed essentially as described by Coen et al. (1990), with slight modifications. Probes for *HvSRN1* and *HvLAX1*, targeting full-length complementary DNAs, were utilized. To prepare the samples, we obtained 8-μm sections from young spikes of seedlings aged 2–6 weeks. These sections were subjected to hybridization with digoxigenin-labeled sense and antisense probes. The resulting signals were observed and captured using an Olympus BX63 microscope equipped with differential interference contrast imaging.

Subcellular localization

To prepare the CaMV35S::SRN-GFP construct, we first obtained the open reading frame (ORF) of *HvSRN1* without a stop codon from R90 cDNA via PCR amplification. The fragment was then inserted into the plant binary vector pCAMBIA1300-GFP and transformed into *Agrobacterium tumefaciens* strain GV3101. This was combined with the p19 strain, which was suspended and mixed in a solution containing 10 mM $MgCl_2$, 10 mM 2-(*N*-morpholino)ethane sulfonic acid, and 150 mM acetosyringone, then incubated at 28°C for 2 h in darkness. *N. benthamiana* leaves were incubated with this mixed suspension for infiltration. After 18–24 h of incubation at 25°C in darkness and 48–72 h under normal conditions, *N. benthamiana* leaves were sampled and used for fluorescence (GFP) visualization. Fluorescence was measured at an excitation wavelength of 488 nm and an emission spectrum of 500–550 nm using a confocal laser scanning microscope (LSM 880).

Plant phenotyping and scanning electron microscopy

Whole barley plants, spikes, and grains were photographed using a Nikon D5600 digital camera. Immature spike tissues at different stages of development were obtained from greenhouse-grown plants and used for scanning electron microscopy as described previously (Bello et al., 2017).

Phylogenetic analysis

A BLASTP search was performed with the amino acid sequence of HvSRN1 to identify its homologous proteins in wheat, rice, maize, and *Arabidopsis* using the NCBI database (https://www.ncbi.nlm.nih.gov/). DNASTAR software was used for multiple sequence alignment with the MegAlign program. MEGA 7.0 (https://megasoftware.net/) was used to construct a neighbor-joining tree of homologous proteins with a maximum-likelihood algorithm and 1000 bootstrap replicates.

Yeast two-hybrid assay

A series of truncated fragments and the full-length ORF of *HvSRN1* were amplified and introduced into an EcoRI-digested pBGKT7 vector. Full-length *HvLAX1* (*HORVU3Hr1G087710.1*) was cloned into an EcoRI-digested pGADT7 vector. Self-activation of HvSRN1 and protein–protein interactions were detected according to the manufacturer's instructions (Clontech, PT4084-1).

LUC activity measurement

To prepare pCAMBIA1300-*HvSRN1*-nLUC, full-length *HvSRN1* (without the stop codon) was amplified and inserted into a KpnI- and SalI-digested pCAMBIA1300-nLUC vector. To construct pCAMBIA1300-cLUC-*HvLAX1*, full-length *HvLAX1* was amplified and inserted into a KpnI- and BamHI-digested pCAMBIA1300-cLUC vector. Both fusion proteins were expressed under the cauliflower mosaic virus 35S promoter. The two constructs were introduced into *A. tumefaciens* strain GV3101. After incubation, the bacterial suspensions were infiltrated into *N. benthamiana* leaves. After a 24-h incubation in darkness and a 48-h incubation under 16 h light and 8 h darkness, LUC activity was measured in the leaves using a low-light cooled CCD imaging apparatus.

Dual-luciferase reporter assay

For promoter activity analysis, a series of mutated *HvSRN1* promoter sequences were cloned into a HindIII- and KpnI-digested pGreenII 0800-LUC vector. To minimize the experimental variability caused by variation in cell activity and transformation efficiency, the Renilla luciferase gene (REN) in the pGreenII 0800-LUC vector was used as an internal transformation control and was activated by the cauliflower mosaic virus 35S promoter. This bacterial suspension was infiltrated into *N. benthamiana* leaves. After 3 days of incubation, the infiltrated leaves were ground into a powder, and their LUC and REN activity was measured with a dual-luciferase reporter assay system (E710; Promega, Madison, WI, USA). The ratio of LUC to REN activity (LUC/REN) was used to determine the activity of the inserted promoter.

Bisulfite sequencing

Bisulfite sequencing was used to profile DNA methylation. Genomic DNA was extracted from young spikes (1–2 mm) of the two parental lines and treated with bisulfite using an EZ DNA Methylation Kit (Zymo Research, Irvine, CA, USA). During this treatment, unmethylated cytosine is converted to uracil, whereas methylated cytosine remains unaffected. The selected promoter region was amplified and sequenced. A fragment of roughly 300 bp was amplified using bisulfite primers and cloned into the pMD19 T-vector, and at least 10 positive plasmid clones were sequenced. The methylation level of the selected region was calculated based on the percentage of cytosine methylation (%C) using the formula 100 × C/(C + T).

Haplotype analysis

Haplotype analysis of *HvSRN1* was performed with 389 domesticated and 56 wild barley accessions. Differences in phenotypic values and haplotypes were examined using one-way ANOVA or Student's *t*-test. The haplotype network was constructed using PopArt 1.7 software (Leigh and Bryant, 2015).

Geographic distribution of two *HvSRN1* alleles

The distribution of two functional types of *HvSRN1* variant was determined in different cultivated barley cultivars. Two competitive allele-specific PCR (KASP) markers (Ksnp-1884 and Ksnp-1748, listed in Supplemental Table 5) were generated using Kraken software (LGC, Biosearch Technologies, Hoddesden, UK). These two markers were used to genotype 525 barley cultivars collected from various regions. Geographic information for the barley cultivars was acquired from the National Crop Genebank of China and was marked on the map to display the geographic distribution characteristics of the two *HvSRN1* alleles.

SUPPLEMENTAL INFORMATION

Supplemental information is available at *Plant Communications Online*.

FUNDING

This work was supported by the National Key R&D Program of China (2018YFD1000706), Hainan Yazhou Bay Seed Laboratory (B21Y10214), the National Natural Science Foundation of China (no. 31771774), the Agricultural Science and Technology Innovation Program, and the China Agricultural Research System (CARS-05).

AUTHOR CONTRIBUTIONS

C.F. drafted the manuscript. C.F., T.D., A.G., Meng Zhao, H.P., Mengwei Zhao, and R.Z. carried out the experiments. K.W. created the CRISPR-Cas9 mutants. G.G., D.X., C.W. and Z.C. revised the manuscript. G.G., Z.N., D.Q., and J.Z. conceived the project and designed the experiments.

ACKNOWLEDGMENTS

The authors declare no conflict of interest.

Received: February 17, 2023
Revised: July 13, 2023
Accepted: August 3, 2023

REFERENCES

Bai, X., Huang, Y., Hu, Y., Liu, H., Zhang, B., Smaczniak, C., Hu, G., Han, Z., and Xing, Y. (2017). Duplication of an upstream silencer of FZP increases grain yield in rice. Nat. Plants **3**:885–893. https://doi.org/10.1038/s41477-017-0042-4.

Beier, S., Himmelbach, A., Schmutzer, T., Felder, M., Taudien, S., Mayer, K.F., Platzer, M., Stein, N., Scholz, U., and Mascher, M. (2016). Multiplex sequencing of bacterial artificial chromosomes for assembling complex plant genomes. Plant Biotechnol. J. **14**:1511–1522. https://doi.org/10.1111/pbi.12511.

Bello, M.A., Ruiz-León, Y., Sandoval-Sierra, J.V., Rezinciuc, S., and Diéguez-Uribeondo, J. (2017). Scanning electron microscopy (SEM) protocols for problematic plant, oomycete, and fungal samples. J. Vis. Exp.55031 https://doi.org/10.3791/55031.

Calderini, D.F., Castillo, F.M., Arenas-M, A., Molero, G., Reynolds, M.P., Craze, M., Bowden, S., Milner, M.J., Wallington, E.J., Dowle, A., et al. (2021). Overcoming the trade-off between grain weight and number in wheat by the ectopic expression of expansin in developing seeds leads to increased yield potential. New Phytol. **230**:629–640. https://doi.org/10.1111/nph.17048.

Chebib, J., and Guillaume, F. (2021). Pleiotropy or linkage? Their relative contributions to the genetic correlation of quantitative traits and detection by multitrait GWA studies. Genetics **219**, iyab159. https://doi.org/10.1093/genetics/iyab159.

Chen, K., Łyskowski, A., Jaremko, Ł., and Jaremko, M. (2021). Genetic and molecular factors determining grain weight in rice. Front. Plant Sci. **12**, 605799. https://doi.org/10.3389/fpls.2021.605799.

Chen, Z., Ke, W., He, F., Chai, L., Cheng, X., Xu, H., Wang, X., Du, D., Zhao, Y., Chen, X., et al. (2022). A single nucleotide deletion in the third exon of FT-D1 increases the spikelet number and delays heading date in wheat (*Triticum aestivum* L.). Plant Biotechnol. J. **20**:920–933. https://doi.org/10.1111/pbi.13773.

Coen, E.S., Romero, J.M., Doyle, S., Elliott, R., Murphy, G., and Carpenter, R. (1990). floricaula: a homeotic gene required for flower development in antirrhinum majus. Cell **63**:1311–1322. https://doi.org/10.1016/0092-8674(90)90426-f.

Comadran, J., Kilian, B., Russell, J., Ramsay, L., Stein, N., Ganal, M., Shaw, P., Bayer, M., Thomas, W., Marshall, D., et al. (2012). Natural variation in a homolog of Antirrhinum *CENTRORADIALIS* contributed to spring growth habit and environmental adaptation in cultivated barley. Nat. Genet. **44**:1388–1392. https://doi.org/10.1038/ng.2447.

de Souza Moraes, T., van Es, S.W., Hernández-Pinzón, I., Kirschner, G.K., van der Wal, F., da Silveira, S.R., Busscher-Lange, J., Angenent, G.C., Moscou, M., Immink, R.G.H., and van Esse, G.W. (2022). The TCP transcription factor HvTB2 heterodimerizes with VRS5 and controls spike architecture in barley. Plant Reprod. **35**:205–220. https://doi.org/10.1007/s00497-022-00441-8.

Ditta, G., Stanfield, S., Corbin, D., and Helinski, D.R. (1980). Broad host range DNA cloning system for gram-negative bacteria: construction of a gene bank of Rhizobium meliloti. Proc. Natl. Acad. Sci. USA **77**:7347–7351. https://doi.org/10.1073/pnas.77.12.7347.

Fischer, R.A. (2011). Wheat physiology: a review of recent developments. Crop Pasture Sci. **62**:95–114. https://doi.org/10.1071/CP10344.

Galli, M., Liu, Q., Moss, B.L., Malcomber, S., Li, W., Gaines, C., Federici, S., Roshkovan, J., Meeley, R., Nemhauser, J.L., and Gallavotti, A. (2015). Auxin signaling modules regulate maize inflorescence architecture. Proc. Natl. Acad. Sci. USA **112**:13372–13377. https://doi.org/10.1073/pnas.1516473112.

Gasparis, S., Przyborowski, M., Kała, M., and Nadolska-Orczyk, A. (2019). Knockout of the *HvCKX1* or *HvCKX3* gene in barley (*Hordeum vulgare* L.) by RNA-guided Cas9 nuclease affects the regulation of cytokinin metabolism and root morphology. Cells **8**:782. https://doi.org/10.3390/cells8080782.

Goetz, M., Rabinovich, M., and Smith, H.M. (2021). The role of auxin and sugar signaling in dominance inhibition of inflorescence growth by fruit load. Plant Physiol. **187**:1189–1201. https://doi.org/10.1093/plphys/kiab237.

Guo, T., Lu, Z.Q., Shan, J.X., Ye, W.W., Dong, N.Q., and Lin, H.X. (2020). *ERECTA1* acts upstream of the OsMKKK10-OsMKK4-OsMPK6 cascade to control spikelet number by regulating cytokinin metabolism in rice. Plant Cell **32**:2763–2779. https://doi.org/10.1105/tpc.20.00351.

Guo, T., Chen, K., Dong, N.Q., Shi, C.L., Ye, W.W., Gao, J.P., Shan, J.X., and Lin, H.X. (2018). *GRAIN SIZE AND NUMBER1* negatively regulates the OsMKKK10-OsMKK4-OsMPK6 cascade to coordinate the trade-off between grain number per panicle and grain size in rice. Plant Cell **30**:871–888. https://doi.org/10.1105/tpc.17.00959.

Hagenblad, J., Leino, M.W., Hernández Afonso, G., and Afonso Morales, D. (2019). Morphological and genetic characterization of barley (*Hordeum vulgare* L.) landraces in the Canary Islands. Genet. Resour. Crop Evol. **66**:465–480. https://doi.org/10.1007/s10722-018-0726-2.

Please cite this article in press as: Fan et al., Natural variations of *HvSRN1* modulate the spike rachis node number in barley, Plant Communications (2023), https://doi.org/10.1016/j.xplc.2023.100670

Harwood, W.A. (2019). An introduction to barley: The crop and the model. Methods Mol. Biol. **1900**:1–5. https://doi.org/10.1007/978-1-4939-8944-7_1.

Higo, K., Ugawa, Y., Iwamoto, M., and Korenaga, T. (1999). Plant cis-acting regulatory DNA elements (PLACE) database: 1999. Nucleic Acids Res. **27**:297–300. https://doi.org/10.1093/nar/27.1.297.

Huang, Y., Kamal, R., Shanmugaraj, N., Rutten, T., Thirulogachandar, V., Zhao, S., Hoffie, I., Hensel, G., Rajaraman, J., Moya, Y.A.T., et al. (2023). A molecular framework for grain number determination in barley. Sci. Adv. **9**, eadd0324. https://doi.org/10.1126/sciadv.add0324.

Jayakodi, M., Padmarasu, S., Haberer, G., Bonthala, V.S., Gundlach, H., Monat, C., Lux, T., Kamal, N., Lang, D., Himmelbach, A., et al. (2020). The barley pan-genome reveals the hidden legacy of mutation breeding. Nature **588**:284–289. https://doi.org/10.1038/s41586-020-2947-8.

Jiao, Y., Wang, Y., Xue, D., Wang, J., Yan, M., Liu, G., Dong, G., Zeng, D., Lu, Z., Zhu, X., et al. (2010). Regulation of OsSPL14 by OsmiR156 defines ideal plant architecture in rice. Nat. Genet. **42**:541–544. https://doi.org/10.1038/ng.591.

Kirby, E.J.M. (1977). The growth of the dhoot apex and the apical dome of barley during ear initiation. Ann. Bot. **41**:1297–1308.

Kirby, E.J.M., and Appleyard, M. (1980). Cytokinin-sensitive genotypes and the control of lateral spikelet development in barley. Maydica **25**:153–168.

Kirby, E.J.M., and Appleyard, M. (1984). Cereal Development Guide, 2nd edn. (Arable Unit, National Agricultural Centre).

Komatsu, M., Chujo, A., Nagato, Y., Shimamoto, K., and Kyozuka, J. (2003). FRIZZY PANICLE is required to prevent the formation of axillary meristems and to establish floral meristem identity in rice spikelets. Development **130**:3841–3850. https://doi.org/10.1242/dev.00564.

Komatsuda, T., Pourkheirandish, M., He, C., Azhaguvel, P., Kanamori, H., Perovic, D., Stein, N., Graner, A., Wicker, T., Tagiri, A., et al. (2007). Six-rowed barley originated from a mutation in a homeodomain-leucine zipper I-class homeobox gene. Proc. Natl. Acad. Sci. USA **104**:1424–1429. https://doi.org/10.1073/pnas.0608580104.

Koppolu, R., Anwar, N., Sakuma, S., Tagiri, A., Lundqvist, U., Pourkheirandish, M., Rutten, T., Seiler, C., Himmelbach, A., Ariyadasa, R., et al. (2013). Six-rowed spike4 (Vrs4) controls spikelet determinacy and row-type in barley. Proc. Natl. Acad. Sci. USA **110**:13198–13203. https://doi.org/10.1073/pnas.1221950110.

Koppolu, R., and Schnurbusch, T. (2019). Developmental pathways for shaping spike inflorescence architecture in barley and wheat. J. Integr. Plant Biol. **61**:278–295. https://doi.org/10.1111/jipb.12771.

Leigh, J.W., and Bryant, D. (2015). POPART: full-feature software for haplotype network construction. Methods Ecol. Evol. **6**:1110–1116. https://doi.org/10.1111/2041-210X.12410.

Li, G., Xu, B., Zhang, Y., Xu, Y., Khan, N.U., Xie, J., Sun, X., Guo, H., Wu, Z., Wang, X., et al. (2022). RGN1 controls grain number and shapes panicle architecture in rice. Plant Biotechnol. J. **20**:158–167. https://doi.org/10.1111/pbi.13702.

Li, N., Xu, R., Duan, P., and Li, Y. (2018). Control of grain size in rice. Plant Reprod. **31**:237–251. https://doi.org/10.1007/s00497-018-0333-6.

Li, S., Zhao, B., Yuan, D., Duan, M., Qian, Q., Tang, L., Wang, B., Liu, X., Zhang, J., Wang, J., et al. (2013). Rice zinc finger protein DST enhances grain production through controlling Gn1a/OsCKX2 expression. Proc. Natl. Acad. Sci. USA **110**:3167–3172. https://doi.org/10.1073/pnas.1300359110.

Li, W., and Yang, B. (2017). Translational genomics of grain size regulation in wheat. Theor. Appl. Genet. **130**:1765–1771. https://doi.org/10.1007/s00122-017-2953-x.

Liang, Y., Liu, H.J., Yan, J., and Tian, F. (2021). Natural variation in crops: Realized understanding, continuing promise. Annu. Rev. Plant Biol. **72**:357–385. https://doi.org/10.1146/annurev-arplant-080720-090632.

Lin, L., Zhao, Y., Liu, F., Chen, Q., and Qi, J. (2019). Narrow leaf 1 (NAL1) regulates leaf shape by affecting cell expansion in rice (*Oryza sativa* L.). Biochem. Biophys. Res. Commun. **516**:957–962. https://doi.org/10.1016/j.bbrc.2019.06.142.

Lin, L., Du, M., Li, S., Sun, C., Wu, F., Deng, L., Chen, Q., and Li, C. (2022). Mediator complex subunit MED25 physically interacts with DST to regulate spikelet number in rice. J. Integr. Plant Biol. **64**:871–883. https://doi.org/10.1111/jipb.13238.

Liu, J., Chen, J., Zheng, X., Wu, F., Lin, Q., Heng, Y., Tian, P., Cheng, Z., Yu, X., Zhou, K., et al. (2017). GW5 acts in the brassinosteroid signalling pathway to regulate grain width and weight in rice. Nat. Plants **3**, 17043. https://doi.org/10.1038/nplants.2017.43.

López, H., Schmitz, G., Thoma, R., and Theres, K. (2021). Super determinant1A, a RAWUL domain-containing protein, modulates axillary meristem formation and compound leaf development in tomato. Plant Cell **33**:2412–2430. https://doi.org/10.1093/plcell/koab121.

Ma, X., Zhang, Q., Zhu, Q., Liu, W., Chen, Y., Qiu, R., Wang, B., Yang, Z., Li, H., Lin, Y., et al. (2015). A robust CRISPR/Cas9 system for convenient, high-efficiency multiplex genome editing in monocot and dicot plants. Mol. Plant **8**:1274–1284. https://doi.org/10.1016/j.molp.2015.04.007.

International Barley Genome Sequencing Consortium, Mayer, K.F.X., Waugh, R., Brown, J.W.S., Schulman, A., Langridge, P., Platzer, M., Fincher, G.B., Muehlbauer, G.J., et al. (2012). A physical, genetic and functional sequence assembly of the barley genome. Nature **491**:711–716. https://doi.org/10.1038/nature11543.

Oikawa, T., and Kyozuka, J. (2009). Two-step regulation of LAX PANICLE1 protein accumulation in axillary meristem formation in rice. Plant Cell **21**:1095–1108. https://doi.org/10.1105/tpc.108.065425.

Sakuma, S., and Schnurbusch, T. (2020). Of floral fortune: tinkering with the grain yield potential of cereal crops. New Phytol. **225**:1873–1882. https://doi.org/10.1111/nph.16189.

Shahinnia, F., Druka, A., Franckowiak, J., Morgante, M., Waugh, R., and Stein, N. (2012). High Resolution Mapping of Dense Spike-Ar (dsp.ar) to the genetic centromere of barley chromosome 7H. Theor. Appl. Genet. **124**:373–384. https://doi.org/10.1007/s00122-011-1712-7.

Skirpan, A., Wu, X., and Mcsteen, P. (2008). Genetic and physical interaction suggest that BARREN STALK1 is a target of BARREN INFLORESCENCE2 in maize inflorescence development. Plant J. **55**:787–797. https://doi.org/10.1111/j.1365-313X.2008.03546.x.

Sreenivasulu, N., and Schnurbusch, T. (2012). A genetic playground for enhancing grain number in cereals. Trends Plant Sci. **17**:91–101. https://doi.org/10.1016/j.tplants.2011.11.003.

Su, S., Hong, J., Chen, X., Zhang, C., Chen, M., Luo, Z., Chang, S., Bai, S., Liang, W., Liu, Q., and Zhang, D. (2021). Gibberellins orchestrate panicle architecture mediated by DELLA-KNOX signalling in rice. Plant Biotechnol. J. **19**:2304–2318. https://doi.org/10.1111/pbi.13661.

Tabuchi, H., Zhang, Y., Hattori, S., Omae, M., Shimizu-Sato, S., Oikawa, T., Qian, Q., Nishimura, M., Kitano, H., Xie, H., Fang, X., Yoshida, H., Kyozuka, J., Chen, F., and Sato, Y. (2011). LAX PANICLE2 of rice encodes a novel nuclear protein and regulates the formation of axillary meristems. Plant Cell **23**:3276–3287. https://doi.org/10.1105/tpc.111.088765.

Tanno, K., Taketa, S., Takeda, K., and Komatsuda, T. (2002). A DNA marker closely linked to the vrs1 locus (row-type gene) indicates multiple origins of six-rowed cultivated barley (*Hordeum vulgare* L.). Theor. Appl. Genet. **104**:54–60. https://doi.org/10.1007/s001220200006.

Thabet, S.G., Moursi, Y.S., Karam, M.A., Börner, A., and Alqudah, A.M. (2020). Natural variation uncovers candidate genes for barley spikelet number and grain yield under drought stress. Genes **11**:533. https://doi.org/10.3390/genes11050533.

Thiel, J., Koppolu, R., Trautewig, C., Hertig, C., Kale, S.M., Erbe, S., Mascher, M., Himmelbach, A., Rutten, T., Esteban, E., Pasha, A., Kumlehn, J., Provart, N.J., Vanderauwera, S., Frohberg, C., and Schnurbusch, T. (2021). Transcriptional landscapes of floral meristems in barley. Sci. Adv. **7**, eabf0832. https://doi.org/10.1126/sciadv.abf0832.

Thirulogachandar, V., Koppolu, R., and Schnurbusch, T. (2021). Strategies of grain number determination differentiate barley row types. J. Exp. Bot. **72**:7754–7768. https://doi.org/10.1093/jxb/erab395.

Thirulogachandar, V., and Schnurbusch, T. (2021). Spikelet stop' determines the maximum yield potential stage in barley. J. Exp. Bot. **72**:7743–7753. https://doi.org/10.1093/jxb/erab342.

Tu, B., Tao, Z., Wang, S., Zhou, L., Zheng, L., Zhang, C., Li, X., Zhang, X., Yin, J., Zhu, X., Yuan, H., Li, T., Chen, W., Qin, P., Ma, B., Wang, Y., and Li, S. (2022). Loss of Gn1a/OsCKX2 confers heavy-panicle rice with excellent lodging resistance. J. Integr. Plant Biol. **64**:23–38. https://doi.org/10.1111/jipb.13185.

van Esse, G.W., Walla, A., Finke, A., Koornneef, M., Pecinka, A., and von Korff, M. (2017). Six-Rowed Spike 3 (VRS3) Is a Histone Demethylase That Controls Lateral Spikelet Development in Barley. Plant Physiol. **174**:2397–2408. https://doi.org/10.1104/pp.17.00108.

Van Ooijen, J.W. (2006). JoinMap® 4, Software for the Calculation of Genetic Linkage Maps in Experimental Populations (Kyazma B.V. Wageningen).

Wang, K., Liu, H., Du, L., and Ye, X. (2017). Generation of marker-free transgenic hexaploid wheat via an Agrobacterium-mediated co-transformation strategy in commercial Chinese wheat varieties. Plant Biotechnol. J. **15**:614–623. https://doi.org/10.1111/pbi.12660.

Wang, Y., Ren, X., Sun, D., and Sun, G. (2015). Origin of worldwide cultivated barley revealed by NAM-1 gene and grain protein content. Front. Plant Sci. **6**:803. https://doi.org/10.3389/fpls.2015.00803.

Wu, Y., Wang, Y., Mi, X.F., Shan, J.X., Li, X.M., Xu, J.L., and Lin, H.X. (2016). The QTL GNP1 encodes GA20ox1, which increases grain number and yield by increasing cytokinin activity in rice panicle meristems. PLoS Genet. **12**, e1006386. https://doi.org/10.1371/journal.pgen.1006386.

Yang, W., Cortijo, S., Korsbo, N., Roszak, P., Schiessl, K., Gurzadyan, A., Wightman, R., Jönsson, H., and Meyerowitz, E. (2021). Molecular mechanism of cytokinin-activated cell division in *Arabidopsis*. Science **371**:1350–1355. https://doi.org/10.1126/science.abe2305.

Yao, H., Skirpan, A., Wardell, B., Matthes, M.S., Best, N.B., McCubbin, T., Durbak, A., Smith, T., Malcomber, S., and McSteen, P. (2019). The barren stalk2 gene is required for axillary meristem development in maize. Mol. Plant **12**:374–389. https://doi.org/10.1016/j.molp.2018.12.024.

Yeh, S.Y., Chen, H.W., Ng, C.Y., Lin, C.Y., Tseng, T.H., Li, W.H., and Ku, M.S.B. (2015). Down-regulation of cytokinin oxidase 2 expression increases tiller number and improves rice yield. Rice **8**:36. https://doi.org/10.1186/s12284-015-0070-5.

Ying, J.Z., Ma, M., Bai, C., Huang, X.H., Liu, J.L., Fan, Y.Y., and Song, X.J. (2018). TGW3, a major QTL that negatively modulates grain length and weight in rice. Mol. Plant **11**:750–753. https://doi.org/10.1016/j.molp.2018.03.007.

Youssef, H.M., Eggert, K., Koppolu, R., Alqudah, A.M., Poursarebani, N., Fazeli, A., Sakuma, S., Tagiri, A., Rutten, T., Govind, G., et al. (2017). VRS2 regulates hormone-mediated inflorescence patterning in barley. Nat. Genet. **49**:157–161. https://doi.org/10.1038/ng.3717.

Zalewski, W., Orczyk, W., Gasparis, S., and Nadolska-Orczyk, A. (2012). HvCKX2 gene silencing by biolistic or Agrobacterium-mediated transformation in barley leads to different phenotypes. BMC Plant Biol. **12**:206. https://doi.org/10.1186/1471-2229-12-206.

Zhai, H., Feng, Z., Li, J., Liu, X., Xiao, S., Ni, Z., and Sun, Q. (2016). QTL analysis of spike morphological traits and plant height in winter wheat (*Triticum aestivum* L.) using a high-density SNP and SSR-based linkage map. Front. Plant Sci. **7**:1617. https://doi.org/10.3389/fpls.2016.01617.

Zhang, X., Jia, H., Li, T., Wu, J., Nagarajan, R., Lei, L., Powers, C., Kan, C.C., Hua, W., Liu, Z., et al. (2022). *TaCol-B5* modifies spike architecture and enhances grain yield in wheat. Science **376**:180–183. https://doi.org/10.1126/science.abm0717.

Zhang, Z., Li, J., Tang, Z., Sun, X., Zhang, H., Yu, J., Yao, G., Li, G., Guo, H., Li, J., et al. (2018). Gnp4/LAX2, a RAWUL protein, interferes with the OsIAA3-OsARF25 interaction to regulate grain length via the auxin signaling pathway in rice. J. Exp. Bot. **69**:4723–4737. https://doi.org/10.1093/jxb/ery256.

Zhao, L., Tan, L., Zhu, Z., Xiao, L., Xie, D., and Sun, C. (2015). PAY1 improves plant architecture and enhances grain yield in rice. Plant J. **83**:528–536. https://doi.org/10.1111/tpj.12905.

Zuo, J., and Li, J. (2014). Molecular genetic dissection of quantitative trait loci regulating rice grain size. Annu. Rev. Genet. **48**:99–118. https://doi.org/10.1146/annurev-genet-120213-092138.

Zwirek, M., Waugh, R., and McKim, S.M. (2019). Interaction between row-type genes in barley controls meristem determinacy and reveals novel routes to improved grain. New Phytol. **221**:1950–1965. https://doi.org/10.1111/nph.15548.